ELECTROSPINNING OF POLYSTYRENE/BUTYL RUBBER BLENDS: A PARAMETRIC STUDY

A THESIS SUBMITTED TO
THE GRADUATE SCHOOL OF NATURAL AND APPLIED SCIENCES
OF
MIDDLE EAST TECHNICAL UNIVERSITY

BY

AHMET GÖKTAŞ

IN PARTIAL FULFILLMENT OF THE REQUIREMENTS
FOR
THE DEGREE OF MASTER OF SCIENCE
IN
CHEMICAL ENGINEERING

FEBRUARY 2008

Approval of the thesis:

ELECTROSPINNING OF POLYSTYRENE/BUTYL RUBBER BLENDS: A PARAMETRIC STUDY

submitted by **AHMET GÖKTAŞ** in partial fulfillment of the requirements for the degree of **Master of Science in Chemical Engineering Department, Middle East Technical University** by,

Prof. Dr. Canan Özgen _____
Dean, Graduate School of **Natural and Applied Sciences**

Prof. Dr. Gürkan KARAKAŞ _____
Head of Department, **Chemical Engineering**

Prof. Dr. Güngör GÜNDÜZ _____
Supervisor, **Chemical Eng. Dept., METU**

Assist. Prof. Dr. Bora MAVİŞ _____
Co-supervisor, **Mechanical Eng. Dept., Hacettepe Univ.**

Examining Committee Members:

Prof. Dr. Savaş KÜÇÜKYAVUZ _____
Chemistry Department, METU

Prof. Dr. Güngör GÜNDÜZ _____
Chemical Engineering Department, METU

Assoc. Prof. Dr. Naime Aslı SEZGİ _____
Chemical Engineering Department, METU

Assoc. Prof. Dr. Halil KALIPÇILAR _____
Chemical Engineering Department, METU

Assoc. Prof. Dr. Necati ÖZKAN _____
Central Laboratory, METU

Date: _____

I hereby declare that all information in this document has been obtained and presented in accordance with academic rules and ethical conduct. I also declare that, as required by these rules and conduct, I have fully cited and referenced all material and results that are not original to this work.

Name, Last name : Ahmet GÖKTAŞ

Signature :

ABSTRACT

ELECTROSPINNING OF POLYSTYRENE/BUTYL RUBBER BLENDS: A PARAMETRIC STUDY

Göktaş, Ahmet

M.Sc., Department of Chemical Engineering

Supervisor: Prof. Dr. Güngör Gündüz

Co-supervisor: Assist. Prof. Dr. Bora Maviş

February 2008, 91 pages

Nanofibers, which have high surface area to volume ratio and better mechanical properties, are nanomaterials that both industry and scientists have started to show great attention in the last two decades. They are used in many areas such as life and filtration sciences, sensors, and composite reinforcement etc.

Among five main production types, electrospinning is the best candidate for further development with a wide range of opportunities to be applied to all types of polymers and ceramics. This method uses electrically charged jet of polymers or liquid states of polymers to produce fibers from micro dimensions down to nano dimensions. Electrospinning setup has mainly three parts; (i) an AC/DC high voltage equipment which creates high electrical potential, (ii) a syringe, and (iii) a collecting screen.

The purpose of this study is to electrospin polystyrene/butyl rubber blends and to investigate the effects of electrospinning parameters on the fibers produced.

In this study, polystyrene/butyl rubber blends were electrospun by changing the applied voltage, the tip-to-collector distance, the flowrate, and the butyl rubber content in the fiber. Finally, morphology of electrospun fibers was characterized by SEM.

The average fiber diameters varied from 760 nm to nearly 10 μm. Increasing butyl rubber content in the fiber resulted in a decrease in the final fiber diameter. Increasing applied voltage also caused a decrease in the final fiber diameter. The tip-to-collector distance did not affect the average fiber diameter. Increasing flowrate yielded fibers with larger diameters. Finally, the addition of non-ionic surfactant decreased the average fiber diameter.

Keywords: Polystyrene, Butyl Rubber, Blend, Electrospinning, Nanofiber

öz

POLİSTİREN/BÜTİL KAUÇUK KARIŞIMLARININ
ELEKTROSPİNLENMESİ: DEĞİŞKENLERİN İNCELENMESİ

Göktaş, Ahmet

Yüksek Lisans, Kimya Mühendisliği Bölümü

Tez Yöneticisi: Prof. Dr. Güngör Gündüz

Ortak Tez Yöneticisi: Yrd. Doç Dr. Bora Maviş

Şubat 2008, 91 sayfa

Yüksek yüzey alan/birim hacim oranına ve üstün mekanik özelliklere sahip olan nanoelyaflar, son yıllarda hem sanayinin hem de bilim dünyasının büyük ilgi gösterdiği nanomalzemeler olmuştur. Bu malzemeler, süzme işlemlerinden yaşam bilimlerine, algaçlardan kompozit takviyesine kadar birçok alanda kullanılmaktadır.

Tüm polimer çeşitlerine ve seramik malzemelere uygulanabilen elektrospinleme yöntemi, bilinen beş ana yöntem içinde daha ileri düzeyde geliştirilebilme şansına sahip olan en iyi adaydır. Bu yöntem elektriksel olarak yüklenmiş polimer jetlerinden ve sıvı fazdaki polimerlerden mikro ve nano boyutlara sahip olan elyaflar üretmek için kullanılmaktadır. Elektrospinleme işlemi üç ana parçadan oluşur, (i) yüksek elektriksel alan yaratan bir yüksek voltaj kaynağı, (ii) bir şırınga ve (iii) bir toplaçtır.

Bu çalışmanın amacı, polistiren/bütil kauçuk karışımlarının elektrospinlenmesi ve elektrospinleme değişkenlerinin etkilerinin araştırılmasıdır.

Bu çalışmada, polistiren/bütil kauçuk karışımlarının elektrospinlenmesi uygulanan voltajın, şırınga ucu ile toplaç arasındaki uzaklığın, jet akış hızının ve karışımdaki bütil kauçuk miktarlarının değiştirilmesiyle elektrospinlenmesi yapılmıştır. Daha sonra, elektrospinleme yöntemiyle elde edilen elyafların morfolojisi taramalı elektron mikroskobu (SEM) yardımıyla incelenmiştir.

Ortalama elyaf çapları 760 nm ile 10 μm arasında değişim göstermiştir. Karışımdaki bütil kauçuk miktarının artması, ortalama elyaf çaplarının azalmasına neden olmuştur. Şırınga ucu ile toplaç arasındaki uzaklığın artırılması üretilen elyafların çaplarında fazla bir değişime neden olmamıştır. Jet akış hızının artırılması elyafların ortalama çaplarının da artmasına yol açmıştır. Karışımlara iyonik olmayan yüzey aktif madde eklenmesi ortalama elyaf çaplarında azalmaya yol açmıştır.

Anahtar sözcükler: Polistiren, Bütil Kauçuk, Karışım, Elektrospinleme, Nanoelyaf.

To My Family

&

My Beloved Mother

ACKNOWLEDGEMENTS

First of all, I would like to express my deepest gratitude to Prof. Dr. Güngör Gündüz for his fantastic supervision, his endless patience, his humanity, his wonderful assistance especially for accepting me as my supervisor and his insightful speech during my thesis research period.

I would also thank to my co-supervisor Ass. Prof. Dr. Bora Maviş for helping me with his great ideas and for his valuable guidance. Additionally, I would like to express my appreciation to Prof. Dr. Üner Çolak for his supports and motivating conversations.

I acknowledge my sincere thanks to Orkun Ersoy from Hacettepe University for helping me on SEM analysis. Prof. Dr. Erdal Bayramlı from Department of Chemistry for giving me the chance to use the instruments in his laboratory and Tuncay Baydemir for his helps in the viscosity measurements and his valuable friendship during my thesis period. I am very thankful to Prof. Dr. Teoman Tinçer giving my the opportunity to use his instruments and his graduate student Şafak Kaya for his help in the density measurements and also many thanks to Nedret Özkar from Central laboratory for Gel Permeation Chromatography (GPC) analysis.

I would like to give my special thanks to my laboratory friends Erkan Biber, Senem Tanrıverdi, Nihan Karakoç, Berker Özerciyes, Özlem Akın, and Esra Güç for their collaborative and friendly manner.

I wish to thank to my work friends A. Pınar Aklan, Özlem Yıldırım, H. Burak Tiftik, Mahmut Bocal, Ertan Öztürk, Eylem Ö.

Nalbantoğlu and the rest for their encouragement and their endless motivation. Additionally, I would like to send my special gratitude to İlter Önder, Didem Özmen, Pınar Kürkçü, Nadiye Gür, Bürge Kılınç, Burcu Koç, Derya Silibolatlaz and all other friends to whom I forgot to write their names here.

I would like to express my most sincere feelings about my family for their unchanged faith from the beginning of my studies, for their pure love with special thanks to Nuray Arslan and Aynure Öztekin's family.

Last but least, I would like to thank all of my other friends for all their emotional assists and motivation during this extremely difficult accomplishment.

TABLE OF CONTENTS

ABSTRACT..... iv
ÖZ.....vi
ACKNOWLEDGEMENTS.....ix
TABLE OF CONTENTS.....xi
LIST OF TABLES.....xiv
LIST OF FIGURES.....xvii
NOMENCLATURE.....xxii
CHAPTER

1.INTRODUCTION.....1
1.1 Nanofibers.....1
1.2 Production Methods.....2
1.2.1 Drawing.....2
1.2.2 Template Synthesis.....3
1.2.3 Phase Separation.....4
1.2.4 Self-Assembly.....5
1.3 Electrospinning.....7
1.3.1 History of Electrospinning Technique.....7
1.3.2 Electrospinning Setup.....8
1.3.3 Electrospinning Process.....9
1.3.4 Parameters Effecting Electrospinning.....12
1.3.4.1 Polymer Solution Parameters.....13
1.3.4.1.1 Solution Conductivity.....13
1.3.4.1.2 Surface Tension.....15
1.3.4.1.3 Dielectric Effect.....16
1.3.4.1.4 Solution Viscosity.....17

1.3.4.1.5 Volatility of the Solvent.....19
1.3.4.2 Polymer Processing Parameters.....20
1.3.4.2.1 Applied Voltage.....21
1.3.4.2.2 Flowrate.....22
1.3.4.2.3 Distance.....23
1.3.4.2.4 Effect of Collector.....23
1.3.4.2.5 Diameter of Needle.....24
1.3.4.3 Ambient Parameters.....25
1.3.4.3.1 Temperature.....25
1.3.4.3.2 Humidity.....26
1.3.4.3.3 Pressure.....27
1.3.4.3.4 Air Velocity and Type of Atmosphere
.....27
1.4 Applications.....28
2. LITERATURE REVIEW.....31
2.1 Electrospinning of Polystyrene.....31
2.2 Electrospinning of Butyl Rubber.....36
2.3 Electrospinning of Polymer Blends and Copolymers Containing Polystyrene.....37
3. EXPERIMENTAL.....40
3.1 Materials.....40
3.1.1 Polystyrene.....40
3.1.2 Butyl Rubber.....41
3.1.3 Tetrahydrofuran (THF).....41
3.1.4 Triton-X 405.....42
3.1.5 Other Materials.....42
3.2 Experimental Procedure.....43
3.2.1 Electrospinning Solution Preparation.....43
3.2.2 Paramaters Investigated.....47
3.2.3 Process Setup and Electrospinning.....47

3.2.4 Heat Treatment.....49
3.3 Characterization Experiments.....49
3.3.1 Viscosity Measurement.....49
3.3.2 Conductivity Measurement.....49
3.3.3 Optical Microscopy.....49
3.3.4 Scanning Electron Microscopy (SEM).....50
3.3.5 Image Analyzer.....50
4. RESULTS AND DISCUSSIONS.....51
4.1 Preliminary Results.....51
4.2 Butyl Rubber Fiber Content in Electrospinning of Polystyrene/Butyl Rubber Blends.....55
4.2.1 Effects of Applied Voltage.....60
4.2.2 Effects of Tip-to-Collector Distance.....63
4.2.3 Effects of Solution Flowrate.....65
4.2.4 Effects of Butyl Rubber Content and Solution Viscosity.....67
4.2.5 Effect of Non-ionic Surfactant Addition.....71
4.2.6 Effect of Sodium Sulphate (Na_2SO_4), Potassium Hydroxide (KOH), and Copper (II) Chloride ($CUCl_2$) Addition.....74
5. CONCLUSIONS.....76
6. RECOMMENDATIONS.....78
REFERENCES.....79
APPENDICES
A. SAMPLE CALCULATIONS.....88
A.1 Sample Calculation for PS/BR Blends in Tables 3.2 to 3.5 88
A.1.1 WV-20/20-90/10.....88
B. GPC ANALYSIS REPORT OF POLYSTYRENE.....91

LIST OF TABLES

TABLES

Table 1.1 Comparison of nanofiber production methods……..…6

Table 1.2 Pore diameters of PS/THF fiber under varying humidity level.....26

Table 2.1 Examples of electrospun polystyrene…….……..32

Table 2.2 Examples of electrospun copolymers and blends including polystyrene…….……38

Table 3.1 Some important properties of THF…….……42

Table 3.2 PS/BR blends prepared from 20 wt % BR …….……..44

Table 3.3 PS/BR blends prepared from 20 wt % PS and 18 wt % BR ……..……44

Table 3.4 PS/BR blends prepared from 20 wt % PS and 15 wt % BR ….……..45

Table 3.5 PS/BR blends prepared from 20 wt % PS and 10 wt % BR……..……..45

Table 4.1 Average fiber and bead diameters of various polystyrene samples electrospun at 10 cm distance, 20 kV applied voltage, and 0.1 ml/min flowrate……55

Table 4.2 Average fiber diameters of polystyrene/butyl rubber blends containing 9.6 % butyl rubber fibers electrospun at 10, 15, and 20 kV applied voltages……61

Table 4.3 Average fiber diameters of polystyrene/butyl rubber blends containing 35 % butyl rubber fibers electrospun at 10, 15, and 20 kV applied voltages……62

Table 4.4 Average fiber diameters of polystyrene/butyl rubber blends containing various (9.6, and 29.5 %) butyl rubber fibers electrospun at 7, 10, and 15 cm working distance……63

Table 4.5 Average fiber diameters of polystyrene/butyl rubber blends containing various (9.6, and 33.8 %) butyl rubber fibers electrospun at the flowrates of 0.05, 0.08, and 0.1 ml/min……65

Table 4.6 Viscosities of PS/BR polymer blends in THF……..68

Table 4.7 Average fiber diameters of polystyrene/butyl rubber blends containing 9.6, 19.3, 27.8, 33.8, 44.6, and 68.6 % BR electrospun at 10 kV applied voltage, 10 cm tip-to-collector distance, and solution flowrate of 0.1 ml/min……71

Table 4.8 Conductivities of PS/BR polymer blends in THF……72

Table 4.9 The average fiber diameters of PS/BR blends containing 24.5 % butyl rubber fibers with 1 % of Triton-X 405……73

Table 4.10 The average fiber diameters of PS/BR blends……..74

LIST OF FIGURES

FIGURES

Figure 1.1 SEM photograph of fibers……2

Figure 1.2 Schematic drawing of electrospinning process……9

Figure 1.3 Schematical view of Taylor Cone…… 10

Figure 1.4 SEM photographs of electrospun nanofibers having different viscosities……18

Figure 1.5 Potential applications of electrospun polymer nanofibers……30

Figure 3.1 Structural formula of polystyrene……40

Figure 3.2 Structural formula of butyl rubber……41

Figure 3.3 Structural formula of THF……41

Figure 3.4 Chemical structure of Triton-X 405……42

Figure 3.5 Schematical representation of preparation of polystyrene and butyl rubber solutions……46

Figure 3.6 Schematical representation of preparation of polystyrene/butyl rubber blend……46

Figure 3.7 Pictures of (a) high voltage power supply and (b) syringe pump……48

Figure 3.8 A representative picture taken during electrospinning……48

Figure 4.1 Optical microscope images of 10 wt % butyl rubber fibers (solvent THF) (a) 15 cm, 15 kV; (b) 15 cm, 20 kV; (c) 15 cm, 25 kV; (d) 20 cm, 15 kV; (e) 20 cm, 20 kV; (f) 20 cm, 25 kV……52

Figure 4.2 SEM images of PS fibers electrospun at 10 cm distance, 20 kV applied voltage, 0.1 ml/min flowrate, and various PS wt concentrations: (a) 10 wt %, (b) 12 wt %, (c) 15 wt %, (d) 18 wt %, and (e) 20 wt %……54

Figure 4.3 Butyl rubber fiber content (wt %) in the total polymer concentration in solution……57

Figure 4.4 SEM images of polystyrene/butyl rubber blends (WV-20/20-50/50, WV-20/18-30/70, WV-20/15-20/80, and WV-20/10-10/90) electrospun at 10 cm tip-to-collector distance, 20 kV applied voltage, and 0.1 ml/min solution flowrate containing (a) 49.1 ;(b) 67.5 ;(c) 75.6 ;(d) 82.7 wt % butyl rubber in the fibers……58

Figure 4.5 SEM images of polystyrene/butyl rubber blends at 10 cm, 20 kV (a) 0.1 ml /min containing 5.6 wt % butyl rubber (WV-20/10-90/10) ;(b) 0.05 ml/min containing 27.8 wt % butyl rubber (WV-20/18-70/30) ;(c) 0.1 ml/min containing 29.5 wt % butyl rubber (WV-20/20-70/30) ;(d) 0.1 ml/min containing 18.3 wt % butyl rubber (WV-20/18-80/20) ;(e) 0.1 ml/min containing 24.5 wt % butyl rubber (WV-20/15-70/30) ;(f) 0.1 ml/min containing 7.9 wt % butyl rubber (WV-20/15-90/10)……59

Figure 4.6 SEM images of polystyrene/butyl rubber blends at 10 cm, 10 kV, and 0.1 ml/min containing (a) 37.5 wt % butyl rubber (WV-20/18-60/40) ;(b) 27.8 wt % butyl rubber (WV-20/18-70/30)….60

Figure 4.7 SEM images of polystyrene/butyl rubber blends (WV-20/20-90/10) containing 9.6 wt % butyl rubber fibers electrospun at 10 cm tip-to-collector distance, and three different applied voltages (a) 10 kV, (b) 15 kV, and (c) 20 kV……61

Figure 4.8 SEM images of polystyrene/butyl rubber blends (WV-20/10-50/50) containing 35 % butyl rubber fibers electrospun at 10 cm tip-to-collector distance, and three different applied voltages (a) 10 kV, (b) 15 kV, and (c) 20 kV……62

Figure 4.9 SEM images of polystyrene/butyl rubber blends (WV-20/20-90/10, WV-20/20-70/30) containing various (9.6, and 29.5 %) butyl rubber fibers electrospun at 20 kV applied voltage, and 0.1 ml/min and three different tip-to-collector distance (a, d) 7 cm, (b, e) 10 cm, and (c, f) 15 cm……64

Figure 4.10 SEM images of polystyrene/butyl rubber blends (WV-20/20-90/10) containing 9.6 % butyl rubber fibers electrospun at 20 kV applied voltage and 10 cm, and three different solution flowrates (a) 0.05 ml/min, (b) 0.08 ml/min, and (c) 0.1 ml/min……...66

Figure 4.11 SEM images of polystyrene/butyl rubber blends (WV-20/15-60/40) containing 33.8 % butyl rubber fibers electrospun at 20 kV applied voltage, and 10 cm and three different solution flowrates (a) 0.05 ml/min, (b) 0.08 ml/min, and (c) 0.1 ml/min……...67

Figure 4.12 The change of viscosity of blend solution with BR content in fiber……..……..69

Figure 4.13 SEM images of polystyrene/butyl rubber blends containing (a) 9.6 %, (b) 19.3 %, (c) 27.8 %, (d) 33.8 %, (e) 44.6 %, and (f) 68.6 % butyl rubber fibers electrospun at 10 kV applied voltage, 10 cm tip-to-collector distance, and solution flowrate of 0.1 ml/min……..……70

Figure 4.14 SEM images of PS/BR blends containing (a) 0 %, (b) 1 % of Triton-X 405. Other values: BR: 24.5, voltage: 20 kV, tip-to-collector distance: 15 cm and solution flowrate: 0.1 ml/min…….73

Figure 4.15 SEM images of PS/BR blends containing (a) BR: 18.7 %, (b) BR: 18.7 % with 1 wt % Na_2SO_4, (c) BR: 27.8 %, (d) BR: 27.8 % with 1 wt % KOH, (e) BR: 9.6 %, and (f) BR: 9.6 % with 1 wt % $CuCl_2$. Voltage: 20 kV, tip-to-collector distance: 10 cm, and solution flowrate: 0.1 ml/min……..…75

NOMENCLATURE

BR	Butyl Rubber
C	Celcius
cm	Centimeter
cP	Centipoise
g	Gram
h	Hour
kV	Kilovolt
MPA	Megapascal
µm	Micrometer
µS	Microsiemens
ml	Milliliter
mm	Millimeter
mmHg	Millimeter Mercury
mPa	Millipascal
min	Minute
nm	Nanometer
PS	Polystyrene
SEM	Scanning Electron Microscope
s	Second
σ	Surface Tension
THF	Tetrahydrofuran

CHAPTER 1

INTRODUCTION

In this chapter, a brief information was given about nanofibers, including definition, applications, and several production methods. Electrospinning process, which is the most popular production method of nanofibers was explained in detail.

1.1 Nanofibers

In general, fibers can be defined as objects or materials that have an elongated structure as shown in **Figure 1.1**. There are other definitions according to the field they are used such as textile industry, biochemistry, physiology, botany, and anatomy. One can call them as nanomaterials, which have a diameter of about 100 nm or less at least in one dimension [1]. In the industry, up to 500nm, it is acceptable to classify fibers with the prefix 'nano' whereas some scientists use the term 'sub-micron' in the academic world. Nanofibers have several superior characteristics. They present a high surface area to volume ratio, better mechanical properties, e.g. good directional strength, and flexibility so they can be utilized for a wide variety of materials and applications including for their mechanical, biomedical, optical, electronical, and chemical properties [2].

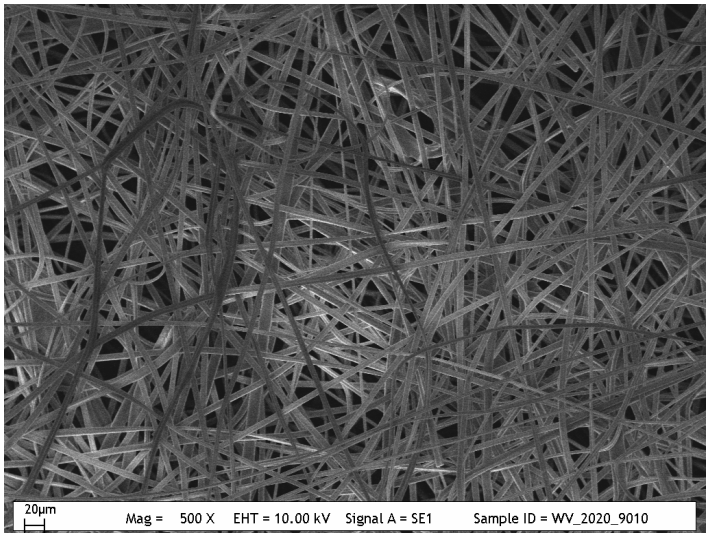

Figure 1.1 SEM photograph of fibers from this study

1.2 Production Methods

There are several processing methods for producing polymeric micro and nanofibers. These are drawing, template synthesis, phase separation, self-assembly, and electrospinning. Among them electrospinning is the best way to produce continuous fibers and the unique one that has a chance to be used in industrial applications.

1.2.1 Drawing

Long single nanofibers can be fabricated by this method. Ondarcuhu and Joachim obtained nanofibers from sodium citrate solution in chloroauric acid by using a micropipette with this method [3]. Harfenist and co-workers drew PMMA fibers from 50 nm to 2 µm. In that study, they used a sharp tip and they dipped the tip into the polymer solution several times in order to get a

consistency in the droplet. Finally, a fiber appears between the tip and the polymer drop [4]. Then the fiber is pulled from its tip end into another liquid solution droplet. With this direct drawing method patterned micro and nanofiber production is possible. However, it is possible to use only for viscoelastic materials. Drawing is advantageous because of minimal use of equipment. On the other hand, being a discontinuous process makes the method impractical.

1.2.2 Template Synthesis

Template synthesis is a way of producing micro- and nanostructures by using nano-scaled diameter membranes. It is thought to be an alternative method to conventional lithography. Desired nanomaterials can be fabricated by adjusting pore diameter of the template. Membranes have cylindrical pores or channels and each of them have diameter uniformly distributed throughout the membrane. This method was first mentioned by Possins and the idea has been developed by Williams and Giordano [5].

In this technique, nanomaterials (nanofibers, nanowires, nanometer-sized fibrils, rods etc.) are prepared by using polymers, conductive polymers, metals, semiconductors, carbons, and other substances. Track-etch and anodic aluminium oxide membranes have been used as templates. However, other nanoporous materials (natural, or man made) and nanostructures can be considered as templates also. There are fundamentally five techniques for template synthesis. These are electrochemical deposition, chemical deposition, chemical polymerization, sol-gel deposition, and chemical vapor deposition (CVD). The template

synthesis method has a number of interesting and useful applications. These nanostructures can have potential usage areas from biomedical sciences to separation technology [6-9]. For example, Feng and his coworkers used template synthesis methodology in their study [6]. They fabricated aligned PAN nanofibers with the average interfiber distance of 513.8 nm and a length of 10.7 μm. They used an anodic aluminium oxide membrane as their template. Schönenberger obtained nanowires of Ni, Co, Cu, Au, and polyparrole in polycarbonate track-etched membrane [5]. They used electrochemical template synthesis technique with a membrane having nominal pore diameters between 10 and 200 nm.

1.2.3 Phase Separation

Nanofibers, nano fibrous matrices, porous 3-D scaffolds, and highly porous foams can be fabricated by phase separation technique. Generally, a polymer is dissolved in its solvent. After dissolution, the mixture is gelated. This procedure is separated into five steps [10]. These are dissolution of polymer, gelation, extraction of solvent, freezing, and freeze-drying under vacuum. They studied the preparation of nano fibrous matrices of some biodegradable polymers (PLLA, PDLLA, and PLGA) and investigated the effects of polymer concentration, thermal treatment, solvent exchange and freezing temperature.

Highly porous foams can be produced by liquid-liquid or solid-liquid phase separation [11, 12]. Thermally induced phase separation has also been in use for the formation of scaffolds for tissue engineering applications. This method includes two phases namely polymer-rich and polymer-lean. The formation of two

phases occurs by cooling or quenching of the polymer solution. In the final step, solvent is sublimed in vacuum or taken away by extraction. Zhang´s study can be given as a sample preparation of foam [12]. In his strategy, he first dissolved 10 ml of PLLA/HAP/dioxane in a beaker at 50°C. The mixture was immediately put into a fridge in order to solidify the solvent. After 2 hrs, liquid nitrogen was used for deep freezing. For dry-freezing, the vessel was kept at -5 °C and -10 °C by using an ice/salt bath. The pressure in the vessel was 0.5 mmHg and after 4 days of treatment solvent was removed fully. At the end, he obtained highly porous polymeric foam. Phase separation is a complex and time consuming process. Type of polymer, type of solvent, polymer concentration, phase separation temperature, thermal treatment, and solvent exchange are the variables of phase separation method. Control on the fiber diameter is difficult and unfortunately, phase separation is limited only to some specific polymers.

1.2.4 Self-Assembly

In self-assembly technique, nanofibers can be derived from single smaller molecules which already exist. These individual molecules organize themselves into desired nano-scale structures. It means that they act as basic building blocks. The idea behind the self-assembly method is that intermolecular forces between those tiny molecules give the overall shape of the resulting nanofibers [13].

Hatgerink and his research team used pH-induced self-assembly [14]. They self-assembled peptide-amphiphile (PA) nano-scale fibrous scaffold which is similar to extracellular matrix. Niece and his coworkers introduced a new approach to self-assembly of

PA [15]. Their study is in contrast with the previous studies which require low pH for self-assembly. There are also other studies carried on this subject [16, 17].

Up to now, four nanofiber production methods have been reported briefly. The fifth one is electrospinning. The comparison between them was given in **Table 1.1**. Among all, electrospinning is the best candidate for further development with a wide range of opportunities to be utilized in all types of polymers (both synthetic and natural), and ceramics. Also, in this thesis study, electrospinning was used for fabrication of non-woven fibers. Therefore, electrospinning process was given in the next section in detail.

Table 1.1 Comparison of nanofiber production methods [13].

Method	Merits	Drawbacks
Drawing	Requires simple equipment	No continuous fibers, no control on fiber dimension
Template Synthesis	Various templates are available for obtaining fibers with different diameters	Process cannot be scaled-up
Phase Separation	Nanofiber matrix fabrication can be done directly	For only specific polymers
Self-Assembly	Nanofiber diameter can be very small (7- 8 nm)	Not controllable on fiber size and complexity of the process
Electrospinning	Long, continuous nanofibers (from cms to meters), has potential for industrial utilization, cost effective	Jet instability

1.3 Electrospinning

Electrospinning, fiber production using electrostatic forces, or electrostatic spinning is described as a novel approach for fiber collection which has become important in the last decades. This method uses electrically charged jet of polymers or liquid states of polymers in order to make fibers from micro dimensions to nano dimensions. In contrast to fibers created from conventional melt spinning, dry spinning or wet spinning, they possess several unique properties. Electrospun fibers are smaller in diameter and longer in length so that they have very high surface area to volume ratios and fibers are placed closer to each other on the mat when compared to fibers produced from dry or wet spinning technologies.

1.3.1 History of Electrospinning Technique

Scientists have begun to realize the great potential in electrospinning in the last fifteen years. This process may be thought as a new technique but it dates back to 1745 when an electrostatic force was applied to a liquid in a glass capillary and aerosol spray had been created [1]. First polymeric filament was patented by Formhals in 1934 [18]. He invented a specific apparatus and produced artificial threads by applying an electrical potential to a polymer solution. In 1952 Vonnegut and Neubauer formed 0.1 mm diameter liquid electrified drops which had uniform shapes [19]. Taylor produced electrified jets by using conducting tubes [20]. After two years from Taylor´s invention, Baumgarten electrospan acrylic fibers in 1971 [21]. In 1997, Fang and Reneker obtained fibers from DNA [22]. Their fibers were around 50 and 80 nm. Then, many other research groups have carried out several

studies related to electrospinning [23-30]. It is obvious that after 1990s, this method was investigated intensively. Still, there is much to understand about the electrospinning process itself.

1.3.2 Electrospinning Setup

Schematic drawing of electrospinning process is given in **Figure 1.2**. The setup has mainly three parts: An AC/DC high voltage equipment which creates high electrical potential, a capillary tube, and a collecting screen. High voltage supplier has two electrodes. One is positive and the other one is negative. In the electrospinning, positive end is attached to polymer solution or polymer melt and negative end is connected to the collecting ground. By adjusting the voltage a required electric field for spinning can be created between the positive and negative sides. Polymer fluid (solution or melt) is filled to a capillary tube where positive electrode wire is inserted into. Capillary tube can be a pipette, micropipette, a glass capillary, a syringe with needle or nozzle. If a metal needle is used for electrospinning, the positive end is wrapped around the metallic needle. Capillary tube position can be vertical with or without using a metering or syringe pump [31]. Polymer fluid holder can be placed horizontally or with various angles [32]. Negative end of the voltage power supplier is connected to a collector opposite to the polymer fluid container. Most fiber collection screens are metallic and covered with an aluminum foil. The shape of the metal collectors is usually flat but in some cases, for specific fiber production (e.g. aligned fibers) dynamic collectors are utilized instead of stationary ones. Rotating drums, discs, or rotating cylindrical collectors are examples of

dynamic screens. Conductive parallel plates are also potential candidates for aligned nanofiber production [33].

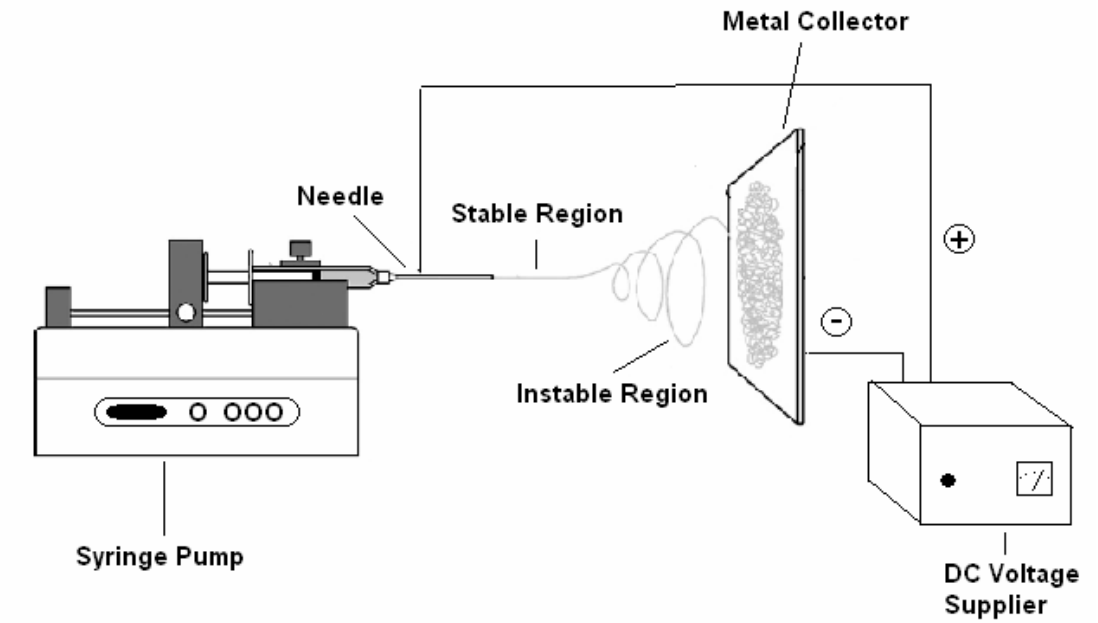

Figure 1.2 Schematic drawing of electrospinning process

1.3.3 Electrospinning Process

Electrospinning process has four different phases. In the first phase, electrically charged liquid polymer jet emerges from the tip of the needle. A whipping process occurs in the second phase. Splaying or multi jet formation is accepted as the third phase and grounding of the thin dried fibers to the collector is the last phase [26]. When an electrostatic force is applied by a high voltage source, an electric field is formed at the tip of the syringe where polymer liquid is held by its surface tension. The accumulation of the charges in the tip causes repulsion which opposes the surface tension forces and the higher the voltage the stronger the mutual

repulsion of the charges at the tip. With the increase of the electric field the pendant polymer drop at the tip of the needle changes its hemispherical shape and takes a conical shape which is called as Taylor cone [20]. A schematical view of the Taylor cone is given in **Figure 1.3**. Taylor stated that a conductive liquid can stay in equilibrium with a cone angle of 49.3° under an electric field. Some recent researches have shown that Taylor cone angle is valid for only to a specific self-similar solution. Cone angle of 33.5° have been reached both experimentally and theoretically with the initiation of a critical electric field [29]. Surface tension can no longer resist mutual repulsive electrostatic forces and charged jet of polymer solution or melt protrudes from the tip of needle at a point of Taylor cone. Polymer jet goes through a short stable region and then immediately gains a chaotic motion or instable region starts. In this region solvent evaporation occurs, leaving a thin dried fiber behind. Fibers are generally collected at the negative polar end as non woven mats.

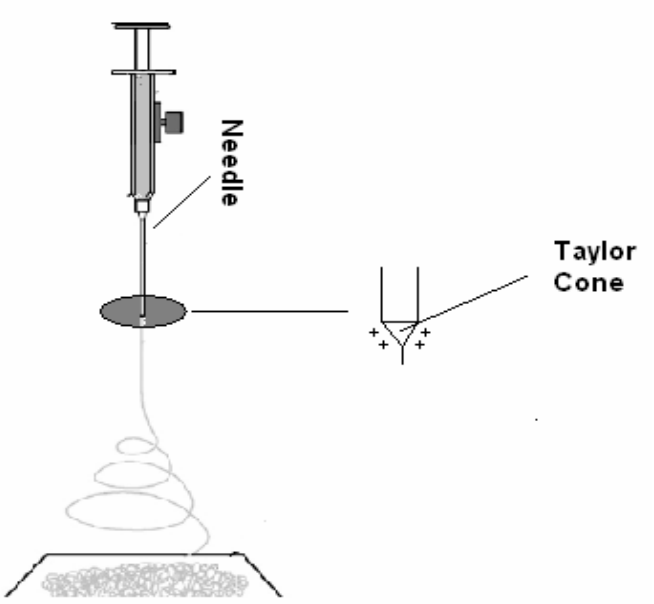

Figure 1.3 Schematic view of Taylor Cone

As previously mentioned, a polymer jet occurs after overcoming the surface tension. Actually, a straight jet is initiated on the surface of the Taylor cone. Straight polymer liquid jet maintains its stability up to a few centimetres [34]. The straight jet path is then followed by an instable area which has a possibility of three models [27]. The classical Rayleigh instability occurs at low charge density, and it yields axisymmetric instability. A second axisymmetric instability which is accepted as a conducting mode occurs at high electric field. A whipping instability which is nonaxisymmetric occurs due to fluctuations in the dipolar component of the charge distributions. These bending instabilities elongate the polymer jet and allow it to bend and stretch. The jet follows an envelope cone road [34]. Polymer jet continues to bend as far as possible after beginning to draw an envelope cone like pathway. Jet splaying or splitting occurs in this area [28, 33]. Multi jet formation from a single polymer fluid results due to high repulsive forces carried by the electrical charges. That means radical forces from electrically charged polymer jets overcome cohesive forces of the jet. Single polymer jet then splits into many other smaller jets before reaching the collector. The jets formed have equal fiber diameter and in each splayed jet, the electrical charge is distributed uniformly. This process causes the resulting fibers to be very thin. Polymer fibers are collected onto a plate or metal screen which is the counter electrode as previously mentioned. Fibers are generally gathered as non-woven filaments [35]. Aligned fibers can also be obtained by using parallel strips. Tan produced aligned polycaprolactone (PCL) ultrafine fibers [36]. Parallel strips were used for their collection. In his study, charged PCL jet travels a path following a bending instability. Dried jet then

catches on one of the strips. The other strip pulls the rest of dried PCL fibers.

There are mainly six types of forces affecting fiber formation according to Wannatong and his research team [37]. His research team concluded that these forces are (i) gravitational or body force, (ii) electrostatic force acting during electrospinning from the tip of the needle to collector, (iii) Coulombic force which has the responsibility of the charged polymer jet stretching, iv) viscoelastic force, which attempts to do just the opposite of what Coulombic force is responsible for, that is trying to stop polymer jet stretching, (v) surface tension which has the same function that the viscoelastic force has, and (vi) drag force which is a result of the friction between the polymer jet and the air in the near vicinity.

1.3.4 Parameters Effecting Electrospinning

In the electrospinning process, the following three parameter classes have relative effects on the resulting fiber properties:

1. Polymer solution parameters
2. Polymer processing parameters
3. Ambient parameters

Solution conductivity, surface tension, dielectric effect, solution viscosity which is closely related to molecular weight of the polymer, solution concentration and polymer chain entanglement, and volatility of the solvent are the properties of the spinning solution. Applied voltage (or electrical potential), flowrate of the polymer solution (or feedrate), diameter of the tip, distance between the tip and the collector, and geometry of collector are the processing parameters. Ambient parameters are thought as

temperature of spinning environment, humidity, air velocity in the media, pressure, and atmosphere around the area [2, 13, 29, 33].

1.3.4.1 Polymer Solution Parameters

Solution parameters of the polymer play the most important role on the morphology of the resultant electrospun fibers. Formation, structure, and size of the beads, and diameter and length of the fibers can be determined by changing these parameters.

1.3.4.1.1 Solution Conductivity

Typical solvents used in electrospinning have low electric conductivities and rarely have some free ions. In electrospinning process, initiation can start only if the solution has enough charges to overcome the surface tension of the polymer solution. Mutual repulsive forces cause the polymer jet to be stretched and this mutual repulsion increases with the increase of charges on the surface of the jet. Addition of ions may enhance the conductivity of a solution. This increase in the conductivity can help production of beadless fibers just because stretching of the solution has increased and to some degree fiber diameter decrease can be observed.

Electrospinning of polystyrene (PS) has been studied in eighteen different solvents [38]. It has been found out that conductivity of the solvent and solution plays an important role in determining the electrospinnability of the polymer solution. Solvents having fair conductivity values seemed to be electrospun better than solvents having no conductivity. It has been observed

that using inorganic salts in the polymer solution has increased the solution conductivity [39]. NaCl, LiCl, and $MgCl_2$ addition caused a monotonic increase in the solution conductivity. However, diameter of the resulting fibers became thicker with increasing the amount of salt. The reason for that was due to the increase in the viscoelastic force and the increase in the mass flow. On the contrary, organosoluble salt addition made a significant reduction on the fiber diameter. Conductivity of the solution increased rapidly with an only small amount of salt but solution viscosity and surface tension were unchanged [40]. Poly(allylamine hydrochloride)(PAH) and poly(acrylic acid sodium salt)(PAA) were used in order to investigate the effect of polyelectrolyte addition to poly(ethylene oxide) solutions [41]. Addition of PAH and PAA caused an increase in the conductivity of the polymer solutions. This rise caused finer and smoother fibers. On the other hand, the effect of conductivity on the fiber diameter was not so strong. The diameter was decreased from 0.36 to 0.2 μm only, and this decrease was limited above a critical value because average diameter of fibers was not directly related to the level of conductivity. Beaded fibers can be vanished by adding small amount of cationic surfactants. Cationic surfactant addition also improves the conductivity of polymer solution. This increase can be seen from the increase in the net charge density of the polymer jet. Stretching of the jet becomes stronger and even a concentration of approximately 10^{-6} mol/l of cationic surfactant was sufficient to stop bead formation in the electrospinning of polystyrene [42].

To sum up, increasing solution conductivity can be done by using conductive solvents, adding ionic (anionic, cationic) or non-

ionic surfactants, organic or inorganic salts, and also adjusting pH of the polymer solution.

1.3.4.1.2 Surface Tension

Surface tension (σ) is defined as force applied to the plane of the surface per unit length. In liquids, a small droplet falling through air takes a spherical shape. Surface property of the liquid which is known as surface tension causes this phenomenon. In electrospinning process, polymer solution has to have sufficient charge in order to overcome surface tension in the liquid solution. During electrospinning, beaded fiber formation can be observed within the polymer jet because of the effect of the high surface tension values. There are various ways to lower the surface tension of the polymer solution. One way is to use solvents having low surface tension. Beaded nanofibers were produced from water/poly(ethylene oxide) solution [25]. Addition of ethanol to the water/poly(ethylene oxide) solution reduced the surface tension of the solution and production of smooth poly(ethylene oxide) nanofibers was obtained. The same effect was found also as in the study of Fong and his research team [43]. They found out that high surface tension causes beaded fibers. Poly(vinylpyrrolidone)(PVP)/N,N-dimethylformamide (DMF) and PVP/dichloromethane (MC) resulted in beaded fibers since they have high surface tension. On the other hand, smooth fibers without bead formation were seen in PVP/ethanol solutions, having a lower surface tension.

Another way is to add surfactant to the spinning solution. Surfactant contribution to the spinning solution is expected to decrease surface tension. Zeng and his coworkers used insoluble

surfactant and observed a decrease in the surface tension [44]. Using soluble surfactants improved fiber formation and decreased the fiber diameter. Insoluble surfactant was even more effective. None or only a slight decrease on the surface tension was observed when a non-ionic surfactant was used. However, cationic surfactants helped in obtaining beadless fibers [42].

1.3.4.1.3 Dielectric Effect

A dielectric material can be defined as material that conducts electricity poorly but supports electrostatic field efficiently. In electrospinning process, solutions with greater dielectric constants are desired because bead formation is reduced and the diameter of the fibers is improved. The relationship between the diameter of resultant fiber and dielectric constant of the polymer solution were studied and at the end of this study, it has been found out that resultant fibers from solutions which have higher dielectric constant have thinner diameter [41]. Net charge density increases when a solution having a higher dielectric constant is used. This causes an increase in the charges along the polymer jet. The elongation of the jet becomes easier with the increase in the charge density under the electrical potential. The decrease in the bead formation and thinner fiber diameter can be explained by this phenomenon. Moreover, using a solvent that has a high dielectric constant enhances the bending instability of the polymer jet. Dielectric constant of the solvents has a significant effect on the productivity of fibers. The correlation between productivity of the resultant fibers and dielectric constant of the solvents is exponential. That means an increase in the productivity is directly related to using a solvent which has a high dielectric constant [37].

1.3.4.1.4 Solution Viscosity

Viscosity of a material can be defined as the measure of the resistance to flow. There are several factors affecting solution viscosity. Molecular weight, polymer chain entanglement, concentration, and temperature are accepted as the main factors. Molecular weight of a polymer is directly related to viscosity of the solution. For the same polymer having different molecular weights, viscosity of the resultant solution will be greater when the polymer which has the higher molecular weight is dissolved by its solvent. Polymer solution has to have the required viscosity, and molecular weight of the polymer must have a value high enough to provide it. This is needed for the fiber production from electrospinning. Otherwise, polymer solution might not produce continuous jets during electrospinning. Continuous jets are obtained with the help of polymer chain entanglements. The amount of polymer chain entanglement is set by the length of the polymer and it is the molecular weight that determines the length of the polymer. The amount of polymer chain entanglement has also an effect on the formation of beads on the fibers. Using higher molecular weight polymers is one of the ways to increase the viscosity and polymer chain entanglement. Increasing the amount of polymer in the solution is another way of increasing the viscosity of the solution. It means that polymer concentration is increased throughout the solution. Increasing solution concentration shows almost same effect as using higher molecular weight polymer. Polymer chain entanglement of the polymer solution is improved in either case. At higher concentrations, viscosity of the solution becomes higher and it prevents the jet having larger bending instabilities. This causes small deposition on the collecting media for fibers and the resultant

fiber diameter is thickened. At low viscosities, there will be less amount of chain entanglement in polymer solution. The forces from surface tension become dominant and bead formation occurs along the string of electrospun fibers. At high viscosities, jets can be stretched fully and beadless fibers can be obtained. This can be observed from **Figure 1.4**. High viscosity values also provoke splitting of jets into smaller fibers. Moreover, pumping of the polymer solution becomes difficult and drying of the solution on the tip of the pipette can be observed.

Figure 1.4 SEM micrographs of electrospun nanofibers having different viscosities [2].

Jarusuwannapoom and his coworkers observed beads at low concentrations [38]. They realized that as the concentration rises in the solution, bead formation becomes less but the resultant fiber diameter increases. It was found out that average diameter of the fibers has an exponential correlation with the viscosity of the solution [39]. The equation is:

$$d = 88.7 + 0.804 \exp(0.00137\mu) \quad (1.1)$$

where,

d = average diameter in nm.

μ = viscosity in cP.

It is stated that increase in the solution viscosity reduces the bead formation but the size of the beads increase and their shape changes from spherical to spindle-like [25]. It was observed that bead density decreases at high viscosity values [45]. Chain entanglement role in the fiber formation during electrospinning was studied [46]. It has been proved that higher than 2.5 entanglements per chain is enough for stable fiber formation. Koski and his research team used six PVAs with different molecular weights ranging from 9000 to 186,000 g/mol in his electrospinning studies [47]. They observed that in each sample a minimum solution concentration is needed for stable fiber formation. Also, another observation was recorded during his studies. Increase in the solution concentration caused increase in the interfiber space and final fiber shape changed from circular to flat.

1.3.4.1.5 Volatility of the Solvent

Solvent volatility is an important factor in electrospinning. Since electrospinning requires a quick evaporation rate and phase separation, vapor pressure of solvent affects the drying time and evaporation rate. There are also other parameters affecting evaporation rate. These are:

- Boiling point
- Specific heat
- Enthalpy and heat of vaporization
- Rate of heat supply

- Interaction between solvent molecules
- Surface tension of liquid
- Air movement above the liquid surface [13]

Solvent volatility is also important in determining the properties of fibrous structures produced by electrospinning. In the electrospinning process, solvent evaporation occurs while the jet travels from the tip of the pipette to the collector. If all of the solvent evaporates on the way, fibers can be formed and deposited on the collector. However, if some solvent still remained on the polymer, instead of dry fibers, wet fibers or thin films can be produced [13, 29].

It is claimed that solvent volatility plays an important role on the formation of pores in the fibers [48, 49]. A decrease in the solvent volatility resulted in smoother fiber surface. However, low boiling point solvents are desirable because evaporation of the solvent is enhanced and deposition of the fibers becomes easier. Matthews and his coworkers chose a volatile solvent having a low boiling point in their study [50]. Solvent volatility can also affect the shape of the fibers produced. Rapid evaporation rate of the solvent can cause the fibers to form as ribbons with various cross sections [31].

1.3.4.2 Polymer Processing Parameters

Processing parameters also influence the electrospinning process. These parameters can be accepted as external factors and they have less significant effects on electrospinning than internal or solution parameters.

1.3.4.2.1 Applied Voltage

Applied voltage determines the amount of charges carried by the jet of the polymer. Therefore, it has been considered quite often. In electrospinning process, when applied voltage reaches a critical value, electrospinning starts from the tip of the needle [50]. Critical voltage is directly correlated with surface tension of the polymer solution. That means applied critical voltage is increased with the increase in surface tension. Their correlation is linear [51]. The shape of the droplet at the tip of the needle can be varied by the increase in the applied voltage. This high voltage also causes more charges in the jet. Increased charge amount leads acceleration in the jet and more solution can be drawn. Applied voltage has also effects on the morphology and the resultant fibers. Increase in the applied voltage results with a decrease in the fiber diameter. Drier fiber can be produced with a high evaporation rate of the solvent. In some cases when the viscosity of the solution jet has a low value, application of high voltage may lead multi jet formation. Hence, thinner fibers can be obtained. Bead formation tendency is also affected by changing voltage. Usually, high voltage results with higher bead formation, but increased jet stretching leads to fewer amounts of beads [38]. At lower voltage, due to the weaker electrostatic force, flight time may last longer. Longer flight time lets the jet to elongate and stretch stronger and longer resulting with reduced fiber diameter. Wang and his research team measured both jet diameter and fiber diameter and investigated the effect of voltage difference [52]. They found out that both jet diameter and fiber diameter decreased slightly. Also, better chain orientation within electrospun fibers was seen by an increase in the

applied voltage. A proportionality relation between applied voltage and fiber diameter was reached in a study [53]. In that study, fiber diameter became thicker as the voltage increased from 5 kV to 25 kV.

1.3.4.2.2 Flowrate

Flowrate is a process parameter that mainly defines the amount of solution that is electrospun into fibers. Fiber deposition can be controlled by varying feedrate. Solution flowrate determines the stability of Taylor cone. It has also influence on bead size and fiber morphology. The increase in the feedrate may result in a relevant increase in the fiber diameter and the bead size. Increasing flowrate leads to an increase in the amount of solution that is electrospun. As a result, residual solvents need more time to be removed. Consequently, jets may not find necessary time to be dried fully. On the collector, some residual solvent can remain and cause fibers to resolve and stick to each other. Four different solution flowrates were used by fixing applied voltage and distance between the tip of the needle and collecting screen to a certain value [54]. Increase in the solution flowrates caused a continuous decrease in the fiber density. Whereas, fiber diameters had a progressive ascending tendency. It has been suggested that bead density can be controlled by arranging appropriate solution flowrates [55]. The jet diameter and the resultant fiber diameter increase were also observed independent of the solvent type [52].

1.3.4.2.3 Distance

The distance between the tip of the needle and the collector has a significant effect on the strength of the electric field and the flying time of the jet throughout electrospinning path. If the distance between two polar ends is short, solvents may not find the required time to be vaporized entirely before the jet arrives at the collector. The resultant fibers may include some solvents left on them. These residual solvents may cause fibers to stick together, and can result in merging of the fibers. Shorter distance between the tip and the collector may lead to an increase in the strength of electric field. This increase accelerates the velocity of the polymer jets. It also reduces the flight time of the polymer jet that is electrospun. Reducing the distance does not affect size and shape of the fibers, but, inhomogeneously distributed beads can be observed [48]. These beads can be due to increase in the electric field strength. If the distance between the tip and the collector is longer, solution jet finds more time for the evaporation of the solvent and jet can be stretched sufficiently before it lands to the collecting media. Increasing the working distance enhances both the number of beads and the density of the fibers [38]. Jet diameter dependence on the working distance is studied [52]. They concluded that increasing working distance caused a decrease on the jet diameter.

1.3.4.2.4 Effect of Collector

In the electrospinning process, usually conductive material is used to cover collecting media. Aluminium foil is one of the most common conductive materials that are used for collection of fibers

onto it. By the help of the conductive material covering, stable potential difference can be obtained between the tip and the collector. Conductive collectors attract more jets on the surface of collector resulting in a higher amount of fiber deposition. For non-conductive collectors, less fiber deposition is seen because charges on the polymer jet flows on the collector due to fast accumulation of the charges. Gathered fibers on the collection area have a lower packing density compared to using a conductive material. Fiber structures and honey comb structures can be obtained by using a non-conducting collective media. Using a porous collector has also an effect on the resulting fibers. The packing density is usually low in porous collectors. This is mainly due to the rate of evaporation of the residual solvents on the fibers deposited. Fiber morphology can be improved by using a dynamic collector. Rotating cylinders are utilized for the production of aligned fibers. One advantage of using rotating collector is that solvents have more time for evaporation.

1.3.4.2.5 Diameter of Needle

In electrospinning process, inner diameter of the needle or pipette also has some effects. Decreasing the inner diameter can cause an observable decrease in:

- Clogging
- The number of beads
- Final fiber diameter

The decrease in the inner diameter creates an increase in the surface tension of the drops on the tip of the needle or pipette. This means that greater amount of electrostatic force is needed to start the formation of a jet. If no voltage changes occur in the process, jet acceleration decreases and gives more time for

stretching and elongating of the jet before it reaches to the collector. Too small inner diameter needle is not desired due to not being able to form droplets at the tip [13]. Zeng and his coworkers studied three different capillary diameters [56]. They found that increasing the internal diameter of the capillary increased both the driving voltage necessary for electrospinning and the diameter of fibers deposited on the collecting mesh.

1.3.4.3 Ambient Parameters

There are not many researches on the effects of ambient parameters. The process and final fiber morphology can be affected by any changes in ambient parameters such as ambient pressure, humidity or temperature. Any electrical force other than the voltage supplier makes changes the electrospinning process so that other parameters on the surrounding may create changes on the resulting fibers.

1.3.4.3.1 Temperature

Rising of the temperature around the spinning environment increases the evaporation rate. Solvent removal from the electrospinning jet becomes easier in a warmer environment. Higher temperature lowers the viscosity of the solution, increases the solubility of the polymer and raises the polymer chain mobility. This greater solubility, low viscosity of the polymer jet and enhanced mobility of the polymer chains strengthen the stretching of the polymer jet and finally more uniform fibers can be produced [56].

1.3.4.3.2 Humidity

Humidity of the surrounding during electrospinning may influence the polymer fluid. It has a direct effect on the surface morphology of the electrospun mats. Pore formation on the surface of the fibers can be seen especially when using volatile solvents. The size and number of the pores increases in high humidity levels. This increase can be easily seen in **Table 1.2**.

Smooth and featureless fibers were seen at humidity values <25 %. Uniform, circular pores were observed at humidity values between 31-38 %. Shape of the pores was same in the humidity range of 40-45 %, whereas their numbers increased heavily. At 50-59 % humidity levels, shape of the pores changed from circular to non-uniform and their size increased dramatically.

Table 1.2 Pore diameters of PS/THF fiber under varying humidity level [57].

humidity range (%)	range of pore diameters (nm)	most frequent pore diameter (nm)
31-38	60-190	85
40-45	90-230	115
50-59	50-270	115
66-72	50-280	135

It was also observed that humidity change does not affect the shape and the diameter of the electrospun fibers.

Evaporation rate of the polymer jet is also affected by the humidity level around the electrospinning area. In low humidity values, polymer jets dry very rapidly due to the high evaporation rate. In some cases, rate of evaporation can be faster than the flowrate of solution from the tip of the needle and finally, clogging of the solution can be observed.

1.3.4.3.3 Pressure

The effect of pressure can be classified into two parts. In the first part, under low pressure conditions (lower than atmospheric pressure), the polymer solution inside of the reservoir has a bigger affinity to flow out. This may result in unstable jet initiation. Further pressure drop causes fast bubbling of the polymer jet. At a critically low pressure, electrospinning can not be accessible due to direct landing of the electrical charges to the collector [13, 58, 59]. When the flowrate of the solution is increased sharply the fibers collected on the screen may be wet. These wet fibers have some residual solvents, and less uniform fibers are obtained [56].

1.3.4.3.4 Air Velocity and Type of Atmosphere

Variations in the atmospheric composition can make significant changes in the electrospinning process. In an electric field gases may show different behaviour from each other. Under helium environment, electrospinning becomes impossible due to the breakdown of helium under high electric field. When spinning is performed under Freon-12 environment, the resultant fibers have a doubled diameter when the same spinning conditions are used. The fibers obtained under Freon-12 atmosphere have also small fibers

"offshoots" from the main fibers [13, 60]. SF_6 atmosphere was also studied for melt electrospinning of PA. Fiber diameters of 900 nm were observed which is very good for melt electrospinning [61]. Air velocity is also an important ambient parameter in electrospinning, but further investigation has to be conducted [62].

1.4 Applications

Nanostructured materials attracted great attention in the last decades. Electrospun nanofibers, having superior properties, have a variety of potential applications. They can be used for filtration processes. In filtration application, nanofibers increase the filter efficiency while providing a low air resistance. In bioengineering science, electrospun fibers are used for biomedical applications such as medical prostheses, tissue template and scaffolds, wound dressing, drug delivery and pharmaceuticals composition, cosmetics, tumor therapy, inhalation therapy, etc. Biocompatibility of the polymers with the body cells is important for biomedical applications and electrospun fibers have to have high surface area and porosity. Nanofibers can also be utilized in defence and security sector. Research on chemical and biological protective clothing has gained much importance in recent years because of the worldwide threats of terrorism. A lightweight and breathable fabric is desirable. This fabric has to be permeable to both air and water vapour, and must be insoluble in all solvents. Since nanofibers have large surface area, they are capable of the neutralization of chemical agents and air and impart water vapour permeability to the clothing. These military protective clothing has sufficient efficiency in trapping aerosol particles by using

nanofibrous mats. Conductive nanofibers are expected to be used for electrical applications. Electrical, ionic, and photoelectric membranes can also be used for electrostatic dissipation, corrosion protection, photovoltaic device, etc. Polymer batteries and polymer capacitors are classified as electrical application devices produced by using conductive electrospun nanostructures. Moreover, sensors, textiles and composite reinforcement are thought as other potential application areas of nanofibers [2, 13, 29, and 61]. The potential applications of polymeric nanofibers are given in **Figure 1.5**.

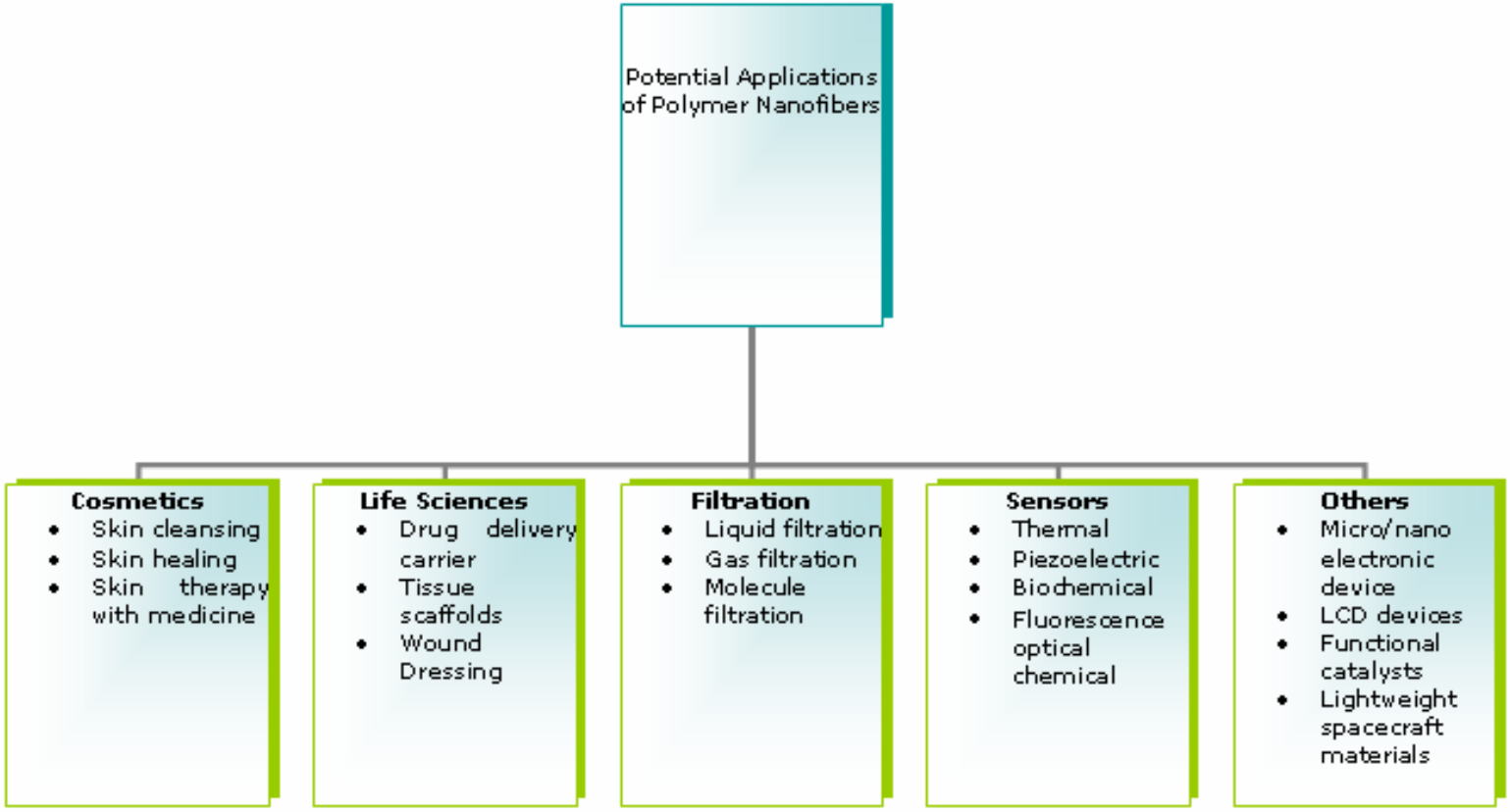

Figure 1.5 Potential applications of electrospun polymer nanofibers [2].

CHAPTER 2

LITERATURE REVIEW

In this chapter, a review about electrospinning of polystyrene, butyl rubber (BR), and polymer blends of polystyrene was introduced briefly. Also, the aim of this study was given shortly.

2.1 Electrospinning of Polystyrene

Polystyrene is one of the commodity polymers that is widely in use today, whereas its first production on an industrial scale dates back 1930s. It is an amorphous thermoplastic polymer which can be processed easily. Polystyrene has a wide variety of applications and uses from household goods to packaging of foods and modification with rubber develops its impact properties [63]. There are many researches carried out related to electrospinning of polystyrene for different purposes. In **Table 2.1**, some examples of electrospun polystyrene are given including solvents and properties of the resulted fibers.

The effect of solvents on electro-spinnability of polystyrene solutions was studied by using eighteen different solvents [38]. Dissolution times of polystyrene pellets varied from 6 hours for Dimethylformamide to 4 days for Decahydronaphthalene. However, toluene was not able to yield a solution which can be electrospun easily even if polystyrene pellets were kept in toluene for seven

days. Solutions were prepared in 10 %, 20 %, and 30 % w/v concentrations and spinning conditions were designed 7, 10, 15 cm as collection distances and 15, 20, 25 kV as applied voltages respectively. Only solutions made with 1,2-dichloroethane, DMF, ethylacetate, MEK, and THF were highly spinnable. It was concluded that high dipole moments and fair conductivity values of these five solvents increase the electro-spinnability of polystyrene solutions.

Table 2.1 Examples of electrospun polystyrene

Polymer	**Solvent**	**Findings**	**Ref.**
Polystyrene Mw:190,000g/mol	THF DMF Chloroform	Porous fiber	[64]
Polystyrene Mw:393,400g/mol	THF Chloroform Carbon disulfide NMP DMF	Dimpled beads (10-20μm) THF, Chloroform, Carbon Disulfide Beads and fibers (~1-5μm) DMF and NMP	[65]
Polystyrene Mn:208,000	THF/DMF (4/0, 3/1,2/2,1/3,0/4)	Porous fibers with diameters of 14.8, 8.7, 7.1, 4.7, and 2.8 μm	[66]
Polystyrene Mw:347,000g/mol	DMF/THF (100/0, 75/25,50/50,25/ 75,0/100)	Min. fiber diameter ⟶ 50-200nm Max. bead diameter⟶20 μm	[49]
Polystyrene Mw:44,100, 393,400, 1,877,000g/mol	THF	Average fiber diameter ~0.5μm & bead-on-string fibers	[67]
Expanded polystyrene	d-limonene	Fiber diameter ⟶ 10-500nm	[68]
Expanded polystyrene	DMAc THF DMF	Fiber diameter ~ 500nm	[69]
Polystyrene Mw:280,000	DMF	Asymmetric Fiber⟶ 1 or 2μm	[31]

The same solvents were also used on the electrospinning of polystyrene solutions in another research [70]. It was observed that the spinnability of the polystyrene solutions depended on their electrical and transport properties as well as their chemical properties. A model was established for electrospinnability. In the model, it has been found that the spinnability is related to the balance of molecular forces at the tip of the needle. Electrical force created from the charges on the polymer solution and gravitational force were driving forces whereas viscous force and the surface tension of the polymer solution were resistant forces. It was also stated that functionalities such as carbonyl groups and nitrogen with free electrons cause high dipole moment and increase the spinnability of polystyrene solutions. Moreover, solvents with viscosities higher than 1.5 cP, fiber production was not successful even at the highest applied voltage (25 kV).

The change in the bead morphology was studied via controlling polymer concentration, applied voltage, and tip-to-collector distance while dissolving polystyrene by using a mixture of solvents tetrahydrofuran (THF) and N,N-dimethyl formamide (DMF) in the ratios 100/0, 75/25, 50/50, 25/75, and 0/100 (v/v) [51]. It has been found out that capillary tip became blocked due to low boiling point of the solvent when using only THF to solve polystyrene. Electrospinning was difficult and large half hollow sphere (HHS) like beads observed which had a diameter around 20-30 μm. The addition of DMF enhanced the electrospinning in addition to eliminating structures other than the fibers. They also concluded that polymer concentration above 15 wt% was enough for forming fibers without beads.

Eda and Shivkumar studied structures of beads in the electrospinning of polystyrene by using THF as solvent [71]. They used six polystyrene having different molecular weights varying from 19,300 g/mol to 1,877,000 g/mol. By controlling molecular weight and polymer concentration, they reached wrinkled, cups, dishes, toroids, and hollow beads.

Polystyrene solutions were electrospun by dissolving it in chloroform at concentrations ranging from 12.5 to 22.5% (w/v), with a flowrate of 0.03 ml/min, and collected the fibers on a rotating mandrel with a rotation speed of 50 to 2000 rpm to produce aligned fibers [53]. In addition, fibers were dried in a vacuum oven at room temperature for evaporation of any residual solvent. A linear relation was found between mean fiber diameter and polymer concentration and the same results were obtained from the relation between mean fiber diameter and applied voltage. However, mean fiber diameter decreased by increasing working distance from 5 to 25 cm.

Six solvents, namely acetic acid, acetonitrile, m-cresol, toluene, THF, and DMF were used to electrospin polystyrene solutions into fibers [37]. The solution with m-cresol could be electrospun at a higher temperature (44 °C) than room temperature (26 °C) due to high boiling point of m-cresol (203 °C). The productivity of electrospun fibers was found high when m-cresol and DMF used as solvents. Fibers from m-cresol and DMF were found less dry than fibers obtained from toluene and THF. The fiber diameters decreased with increasing solvent content and boiling point. The thinnest fibers (200 nm) were obtained from 27 % (w/v) of polystyrene in m-cresol. They concluded that best solvent was DMF and the fibers from its solution were found to

have the highest productivity, without beads, well-aligned and optimal morphological characteristics. Polystyrene fibers with a diameter of 700 nm were produced from the solution of 10 % (w/v) at an applied voltage of 15 kV, with 10 cm tip-to-collector distance, at a nitrogen flowrate of 101 ml/min, and a rotational collector with a rotation speed of 1500 rev/min.

Cationic surfactants, dodecyltrimethyl ammonium bromide (DTAB) or tetrabutylammonium chloride (TBAC) and a non-ionic surfactant, were used in the polystyrene solutions [42]. The solutions were prepared by using equal volume of both DMF and THF with a concentration range of 5-15 % (w/v). Adding only a small amount of cationic surfactant resulted with no bead formation during electrospinning. Cationic surfactant addition caused an observable increase in the solution conductivity but no change in the solution viscosity. Surface tension of the polymer solution slightly decreased by the addition of DTAB. On the other hand, the addition of Triton X-405 did not eliminate the beaded fibers only a decrease was observed in the number of beads.

Four solvents (DMF, o-dichlorobenzene (o-DCB), THF, and chloroform(CF)) and three salts (triethylbenzylammonium chloride (TEBAC) for DMF and CF, tetra-n-butylammonium perchlorate (TBAPC) for o-DCB, and lithium perchlorate ($LiClO_4$) for THF solutions were used to electrospin polystyrene [52]. It has been found that as the flowrate and solution viscosity increase, solution jet and the final fiber diameter also increase. The increase in solution conductivity and applied voltage caused a decrease in solution jet and deposited fiber diameters, but this decrease was very slight in voltage case. Moreover, addition of salts improved the final fiber properties and morphologies.

2.2 Electrospinning of Butyl Rubber

Butyl rubber is a synthetic rubber, or elastomer which is also known as polyisobutylene. It is produced by polymerization of about 98% of isobutylene and 2 % of isoprene. Polyisobutylene is the only rubber that is gas impermeable. [72] Electrospinning of butyl rubber solutions has not been widely studied yet. There are few publications on it. Butyl rubber suggests good mechanical response properties and is utilized in chemical protective clothing applications. However, it has no breathability.

Viriyabanthorn and his coworkers reported electrospinning of butyl rubber compounds and studied the effect of carbon black loading on the final fiber morphology [73]. They used four different carbon black loading levels. THF was the solvent used in the experiments. It was difficult to obtain fibers without carbon black loading. At higher viscosities, butyl rubber fibers were produced but they lost their shape before evaporation of residual solvent was terminated. They concluded that increased carbon black loading enhanced the processing conditions for preparation of microporous butyl rubber fibers and decreased the bead formation and fiber diameter.

The electrospinning of butyl rubber and effects of the type of carbon black were also studied [74]. It was used a sulphur cured butyl rubber compound and eight different types of carbon black, each having different particle size and structure in the study. THF was the solvent used in the electrospinning process. The flowrate was 1 ml/min and fibers were deposited on a rotating collector. The experiments demonstrated that increasing carbon black particle size caused an increase in the fiber diameter. Increasing carbon

black caused an increase in the conductivity of the polymer solution and thus decreased the fiber diameter. They found out that concentration of the solution plays an important role in determining fiber diameter and formability.

2.3 Electrospinning of Polymer Blends and Copolymers Containing Polystyrene

Kalra and his coworkers synthesized poly (styrene-block-isoprene) and obtained fibers by using electrospinning method [75]. They used THF as solvent, and produced fibers which have fiber diameters from 200 nm to 5 μm.

Two thermoplastic elastomers based on block copolymers of styrene and isoprene was electrospun [76]. These copolymers were multi-armed poly (styrene-b-isoprene) and linear poly (styrene-b-isoprene-b-styrene). 1,2-dichloroethane and chloroform were the solvents used in this research. They investigated the effect of solution concentration, applied voltage, solution flowrate, and chemical structures of the electrospun copolymers. They found that the increase in the solution concentration increased the electrospinnability of both polymers. The diameter of the resulting fibers first decreased, and then reached a minimum value, after that started to increase again under increasing applied voltage. The average diameter of the fibers was found to increase with increasing solution flowrate. The effect of chemical structure was found that the poly (styrene-b-isoprene) fibers had a larger diameter than the fibers of poly(styrene-b-isoprene-b-styrene) even though they had same viscosity values.

Ji and his research team performed a research on the electrospinning of polystyrene/clay nanocomposite fibers [77]. They obtained fibers ranging from 150 nm to 4 μm by changing solution concentration. The addition of clays produced fibers with a highly aligned montmorillonite layer structure. The higher clay addition yielded agglomeration.

In **Table 2.2**, some other fibers from polymer blends and copolymers containing polystyrene by electrospinning process are presented.

Table 2.2 Examples of electrospun copolymers and blends including polystyrene

Polymer	Solvent	Findings	Ref.
Polyaniline/Polystyrene Mw:65,000/280,000g/mol	Chloroform THF	Core and Sheath nanofibers	[78]
Tetrabutyl titanate/Polystyrene	THF DMF	Sol-gel processing Fiber diameter ⟶ 200-550 nm	[79]
Polystyrene/MEH-PPV, 7.5:1, 15:1, 22.5:1	Chloroform 1,2-dichloroethane	Organic salt addition (Pyridinium formate) Fiber diameter⟶ 0.30-5.11 μm	[80]
SWNT-filled polystyrene composites	DMF	Fiber diameter ⟶ 50-100 nm	[81]
Poly(Styrene-b-dimethylsiloxane)	THF:DMF 3:1	Fiber diameter ⟶150-400 nm	[82]
HCSA doped-PANI /Polystyrene	Chloroform	Fiber diameter ⟶ 400-1000 nm	[83]
Polystyrene latex/ PVA	Water	Non-ionic surfactant (Basensol) Fiber diameter ⟶ 100-900 nm	[84]
PS-b-PPG	DMF	Fiber diameter ⟶ 0.25-2.20 μm	[85]

Up to the present, as far as is known, there has been no published study on the electrospinning of polystyrene/butyl rubber blends in the literature. In this study, the aim was to electrospin polystyrene/butyl rubber blends together and to increase flexibility and toughness of polystyrene by adding butyl rubber. Therefore, polystyrene/butyl rubber blends were electrospun by changing applied voltage, tip-to-collector distance, flowrate, and polymer concentration parameters. Finally, morphology of electrospun fibers was characterized by SEM.

CHAPTER 3

EXPERIMENTAL

3.1 Materials

3.1.1 Polystyrene

Polystyrene pellets were supplied by PETKİM. The molecular weight of the polystyrene pellets was measured at the Central Laboratory of Middle East Technical University (METU) by using a Gel Permeation Chromatography (PL-GPC 220), and found to be 135,000 g/mol (M_w). The density of polystyrene was found as 1.03 g/cm^3. The measurement was done by using a picnometer. The chemical structure of polystyrene is presented in **Figure 3.1**.

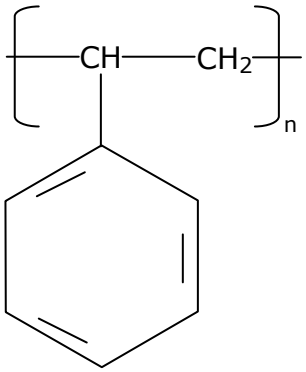

Figure 3.1 Structural formula of polystyrene

3.1.2 Butyl Rubber

Butyl rubber or polyisobutylene, which was used as a polymer and also in polymer blends of polystyrene/butyl rubber for electrospinning, was supplied from Goodyear Lastikleri T.A.Ş. The density of butyl rubber was found as 0.864 g/cm^3. The measurement was carried out by using an Electronic Densimeter (MD-300S). The chemical structure of butyl rubber is given in **Figure 3.2**.

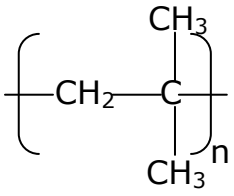

Figure 3.2 Structural formula of butyl rubber

3.1.3 Tetrahydrofuran (THF)

THF was used to solve polymers and to prepare solutions for electrospinning. THF was purchased from Merck KGaA, Germany. Some basic properties and chemical structure of THF are given in **Figure 3.3** and **Table 3.1** respectively.

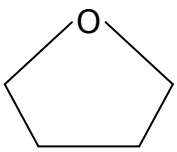

Figure 3.3 Structural formula of THF

Table 3.1 Some important properties of THF [86].

Property	Magnitude	Unit
Molecular Weight	72.11	g/mol
Density (at 20 °C)	0.89	g/cm^3
Melting point	-108.50	°C
Boiling point	65-66	°C
Viscosity (at 20 °C)	0.48	mPa.s
Solubility Parameter	19.40	$MPa^{1/2}$

3.1.4 Triton-X 405

Triton-X 405, 70 % solution was used as a non-ionic surfactant in this study. Triton-X 405 was purchased from Aldrich, USA. Chemical structure of this non-ionic surfactant is given in **Figure 3.4**.

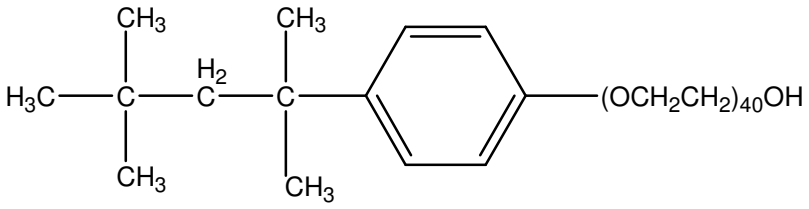

Figure 3.4 Chemical structure of Triton-X 405.

3.1.5 Other Materials

Potassium hydroxide (KOH), a very alkaline and strong base, used in this study was purchased from Merck, Darmstadt, Germany. Sodium sulphate (Na_2SO_4), sodium salt of sulphuric acid, was

purchased from Riedel-De Haen Ag Seelze, Hannover. Copper (II) chloride ($CuCl_2$) used in this study was purchased from Merck, KGaA, Germany.

3.2 Experimental Procedure

3.2.1 Electrospinning Solution Preparation

In this study, polystyrene, butyl rubber and different compositions of these polymer solutions were prepared by using THF as solvent. For the preliminary part, butyl rubber and polystyrene solutions were prepared by varying weight-to-volume (w/v) compositions. Butyl rubber compositions in THF were 5 wt%, 10 wt%, and 15 wt%. Polystyrene compositions in THF were 10 wt%, 12 wt%, 15 wt%, 18 wt%, and 20 wt%. In a typical experiment, both polystyrene and butyl rubber were dissolved separately to form a clear solution within one day in THF. Then, the mixture was vigorously stirred overnight at room temperature by using a magnetic stirrer in order to obtain a homogeneous solution.

For polymer blend preparation, polystyrene and butyl rubber again were dissolved separately in THF. They were kept in different flasks at room temperature. Before electrospinning process, the determined amounts of both polymers (i.e. polystyrene and butyl rubber) were mixed and then the mixture was stirred around 1 hour on a magnetic stirrer. Surfactant and other materials were also added at this step. That is, just before stirring has been started. In all blends, polystyrene solutions were 20 wt%. Four different weight percentages of butyl rubber solutions were utilized in the experiments. These were 10 wt%, 15 wt%, 18 wt%, and 20 wt%. The weight compositions of the prepared materials are listed

in **Table 3.2**, **Table 3.3**, **Table 3.4**, and **Table 3.5**. Sample conversion calculation from v/v % to wt/wt % for PS/BR blends in **Tables 3.2** to **3.5** is given in **Appendix A**.

Table 3.2 PS/BR blends prepared from 20 wt% PS and 20 wt% BR.

WV-20/20 (v/v) PS/BR (ml/ml) (%)	**PS (g) (%)**	**BR (g) (%)**	**Total Polymer Conc. (g) (%)**
90/10	15.1	1.6	16.7
80/20	13.4	3.2	16.6
70/30	11.7	4.9	16.6
60/40	10.0	6.5	16.5
50/50	8.4	8.1	16.5

Table 3.3 PS/BR blends prepared from 20 wt% PS and 18 wt% BR.

WV-20/18 (v/v) PS/BR (ml/ml) (%)	**PS (g) (%)**	**BR (g) (%)**	**Total Polymer Conc. (g) (%)**
90/10	15.1	1.5	16.6
80/20	13.4	3.0	16.4
70/30	11.7	4.5	16.2
60/40	10.0	6.0	16.0
50/50	8.4	7.4	15.8
40/60	6.7	8.9	15.6
30/70	5.0	10.4	15.4

Table 3.4 PS/BR blends prepared from 20 wt% PS and 15 wt% BR.

WV-20/15 (v/v) PS/BR (ml/ml) (%)	PS (g) (%)	BR (g) (%)	Total Polymer Conc. (g) (%)
90/10	15.1	1.3	16.4
80/20	13.4	2.6	16.0
70/30	11.7	3.8	15.5
60/40	10.0	5.1	15.1
50/50	8.4	6.4	14.8
40/60	6.7	7.7	14.4
30/70	5.0	8.9	13.9
20/80	3.3	10.2	13.5

Table 3.5 PS/BR blends prepared from 20 wt% PS and 10 wt% BR.

WV-20/10 (v/v) PS/BR (ml/ml) (%)	PS (g) (%)	BR (g) (%)	Total Polymer Conc. (g) (%)
90/10	15.1	0.9	16.0
80/20	13.4	1.8	15.2
70/30	11.7	2.7	14.4
60/40	10.0	3.6	13.6
50/50	8.4	4.5	12.9
40/60	6.7	5.4	12.1
30/70	5.0	6.3	11.3
20/80	3.3	7.2	10.5
10/90	1.7	8.1	9.8

The outline of the experimental procedure for the preparation of polystyrene or butyl rubber is illustrated in **Figure 3.5**, and mixture of both polymers is illustrated in **Figure 3.6**.

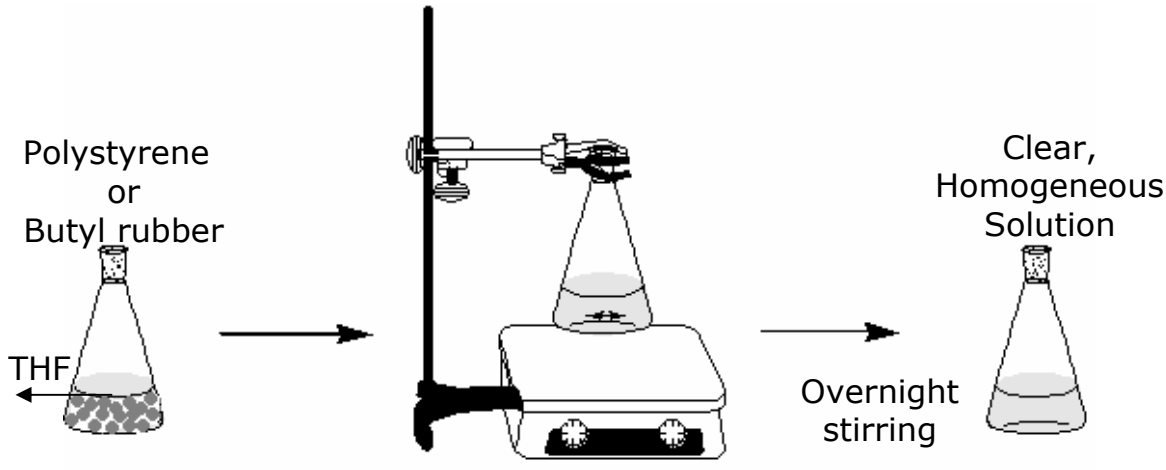

Figure 3.5 Schematical representation of preparation of polystyrene and butyl rubber solutions.

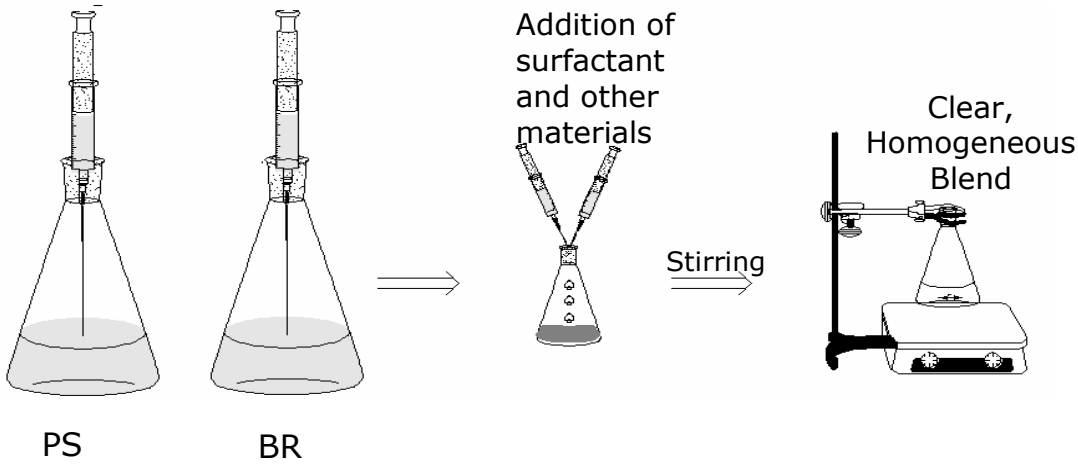

Figure 3.6 Schematical representation of preparation of polystyrene/butyl rubber blends.

3.2.2 Parameters Investigated

Three different process parameters were investigated in this study. These were applied voltage, tip-to-collector distance, and solution flowrate. The applied voltages were 10 kV, 15 kV, and 20 kV. The tip-to-collector distances were selected as 7 cm, 10 cm, and 15 cm. The flowrates used for the electrospinning process were 0.05 ml/min, 0.08 ml/min, and 0.10 ml/min. The total polymer concentration varied from 9.8 wt% to 16.7 wt% which was represented previously in **Tables 3.2 to 3.5**.

3.2.3 Process Setup and Electrospinning

In electrospinning process, the setup consisted of a DC high voltage power supply seen in **Figure 3.7 (a)** from GAMMA High Voltage Research Inc., USA (Model no: ES30P-20W/DAM) with an electrical potential range from 0 to 30 kV, and a multi-syringe pump seen in **Figure 3.7 (b)** (New Era Pump Systems Inc. Model no: NE-1600 Six-Syringe Pump). The flowrate can range from 0.568 µL/hr (1 ml syringe) to 1337 ml/hr (60 ml syringe). We have used 10 ml syringe with a needle diameter of 0.8 mm supplied by Ayset A.Ş. (Adana, Türkiye). The metal collector was covered with an aluminum foil. The setup was kept in a plexiglass box for experimenter's safety. All experiments were carried out under atmospheric pressure and at room temperature. The positive electrode wire was hooked at the metal part of the needle and negative part of the electrode was attached to the metal collector. Five to ten minutes of operation time was sufficient for the deposition of fibers on aluminum foil. A horizontal setup was

chosen for electrospinning process. A picture that was captured during electrospinning is illustrated in **Figure 3. 8**.

(a)

(b)

Figure 3.7 Pictures of (a) high voltage power supply and (b) syringe pump

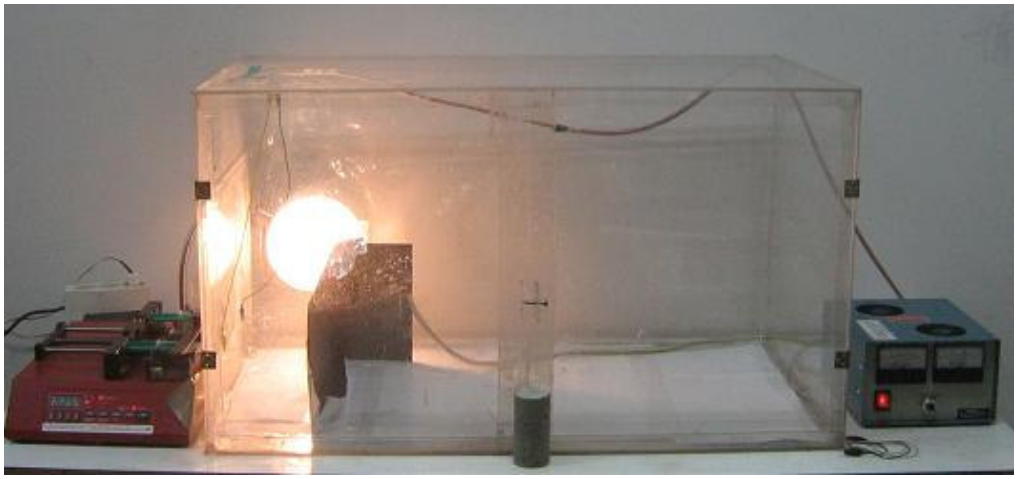

Figure 3.8 A representative picture taken during electrospinning

3.2.4 Heat Treatment

Fiber samples were kept in an oven just after electrospinning process. The oven temperature was set to 60 °C and the samples were kept there for 24 h in order to remove any residual solvents in fibers.

3.3 Characterization Experiments

3.3.1 Viscosity Measurement

The viscosities of the polymer blend solutions were measured by using a Brookfield viscometer (Model DV-II). The measurements were done under atmospheric pressure and at room temperature. Spindle rotation speed was fixed at 100rpm. Three measurements were taken for each sample.

3.3.2 Conductivity Measurement

The conductivity measurement of the polymer solution samples was performed by using a Jenco conductometer (Model 3250). The calibration was performed by two points with KCl standard solution before measurements. Three measurements were taken for each sample.

3.3.3 Optical Microscopy

The micrographs of electrospun butyl rubber fibers were obtained by using an optical microscope (Prior Scientific Instruments Ltd. England, Model: 4200) equipped with an image

analyzer (Pro-Series, High Performance CCD). The optical microscope was used for preliminary studies only.

3.3.4 Scanning Electron Microscopy (SEM)

The electrospun fibers were characterized by a scanning electron microscope (Model: Zeiss Evo 50 VP). The majority of SEM images were taken at 500x and 3000x magnifications.

3.3.5 Image Analyzer

The diameter of fibers was determined by using an image analyzer software program called ImageJ. It is a Java-based image-processing program which can analyze, process, and read many image formats including TIFF, PNG, GIF, JPEG etc. 20-30 samples were chosen for each SEM image depending on the number of availability.

CHAPTER 4

RESULTS AND DISCUSSIONS

In this chapter, the results of the experiments including the preliminary ones, were given and discussed by using SEM micrographs.

4.1 Preliminary Results

Butyl rubber was first electrospun by preparing 5 wt%, 10 wt%, and 15 wt% solutions in THF. Butyl rubber solution having a concentration of above 15 wt% was not suitable for electrospinning due to its high viscosity. Solution with butyl rubber content less than 5 wt% was also not suitable for electrospinning due to low viscosity. We found out that 10 wt% of butyl rubber solutions were electrospinnable. Therefore, 10 wt% of solutions were electrospun at different applied voltages, and different tip-to-collector distances. **Figure 4.1** represents optical microscope pictures of these electrospun butyl rubber fibers. As it can be observed from the micrographs, uniform fiber formation was difficult to achieve. Fibers merged together and bead formation took place.

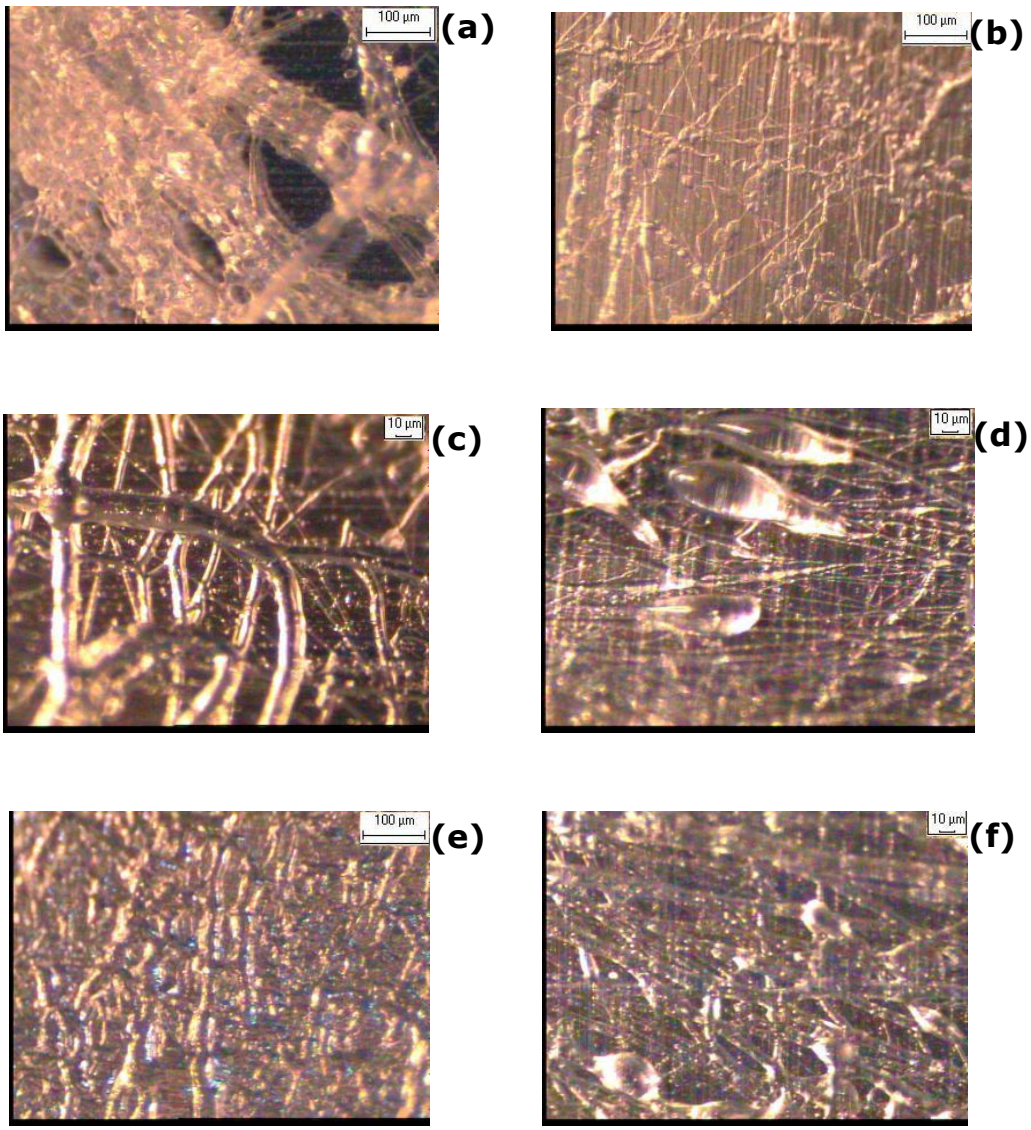

Figure 4.1 Optical microscope images of 10 wt% butyl rubber fibers (solvent THF) **(a)** 15 cm, 15 kV; **(b)** 15 cm , 20 kV; **(c)** 15 cm , 25 kV; **(d)** 20 cm, 15 kV; **(e)** 20 cm, 20 kV; **(f)** 20 cm, 25 kV.

In fact butyl rubber is not the best polymer as far as the electrospinning technique has been considered. There is only one example of electrospinning of butyl rubber with other compounds, namely carbon black [73, 74]. Since butyl rubber is an extremely

flexible material, we prepared its blend with polystyrene which is a quite rigid polymer and then electrospun these blends. Thus, the blends of the two can demonstrate an increased toughness compared to the polystyrene only. Therefore, another group of preliminary experiments were carried out with the help of literature data on the electrospinning of polystyrene. Polystyrene can dissolve in many solvents [38]. However, dissolution of butyl rubber can not be easily achieved. Aromatic hydrocarbons, such as hexane, octane, etc. can dissolve butyl rubber but polystyrene is not soluble in them. THF was found to be the solvent that can dissolve both of the polymers, and therefore it was used as the only solvent in this study.

Five different polystyrene concentrations were used to produce fibers without bead formation: 10 wt%, 12 wt%, 15 wt%, 18 wt%, and 20 wt%. The fibers produced from them are shown in **Figure 4.2**. Fibers without beads were seen only in 20 wt%. On the other hand, as polymer concentration increased the diameter of the fibers increased but the number of beads were decreased. The average fiber diameters and some other properties of electrospun polystyrene samples are given in **Table 4.1**.

Thus, 20 wt% polystyrene concentrations were used in all other experiments including electrospinning of polystyrene/butyl rubber blends.

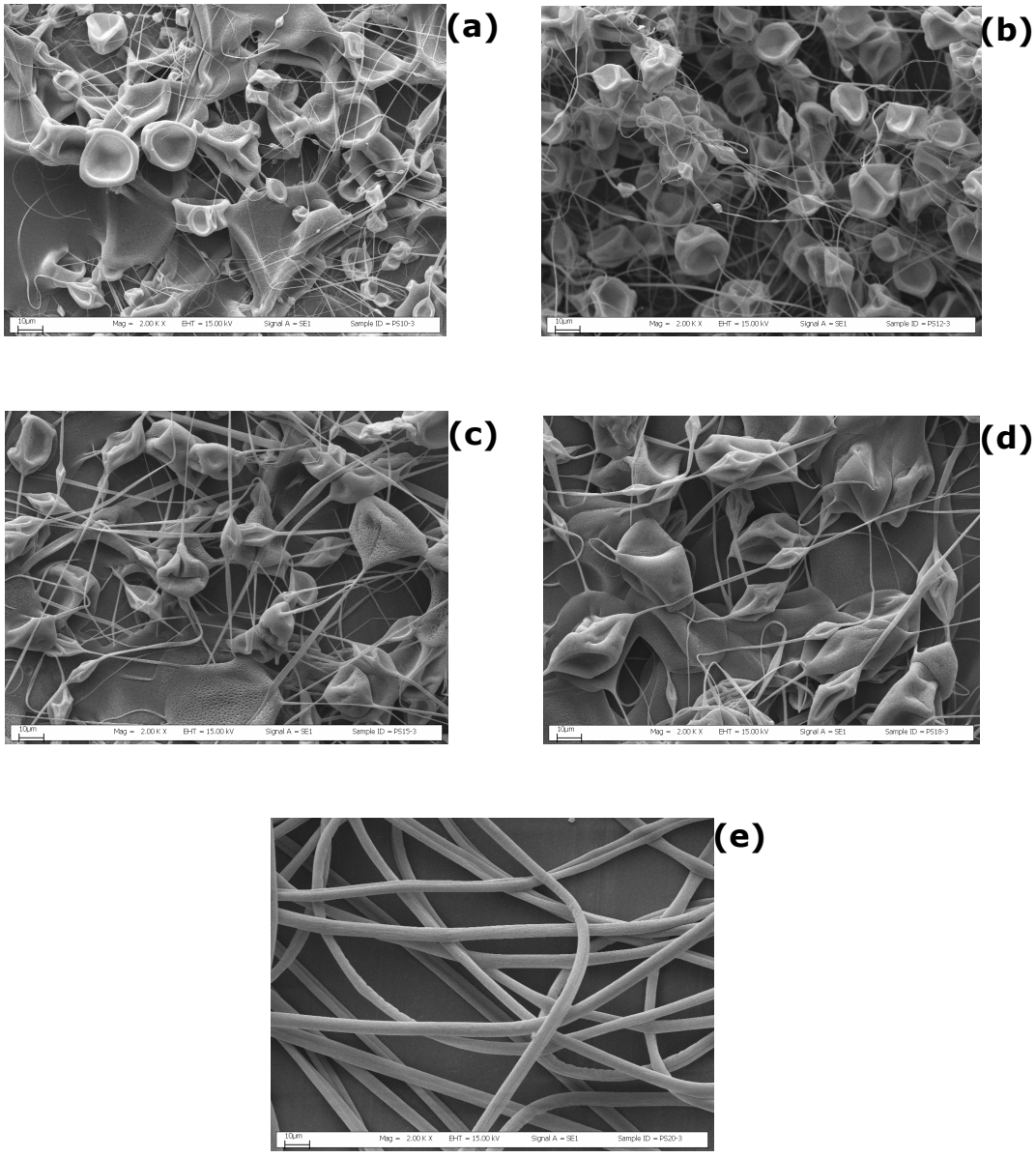

Figure 4.2 SEM images of PS fibers electrospun at 10 cm distance, 20 kV applied voltage, 0.1 ml/min flowrate, and various PS wt concentrations: **(a)** 10 wt%, **(b)** 12 wt%, **(c)** 15 wt%, **(d)** 18 wt%, and **(e)** 20 wt%.

Table 4.1 Average fiber and bead diameters of various polystyrene samples electrospun at 10 cm distance, 20 kV applied voltage, and 0.1 ml/min flowrate.

Polystyrene (wt%)	Average fiber diameter (μm)	Average bead diameter (μm)	Minimum fiber diameter (μm)	Maximum fiber diameter (μm)
10	0.50±0.20	8.40±6.80	0.20	0.90
12	0.70±0.20	14.00±4.60	0.30	1.40
15	1.10±0.50	9.60±3.80	0.30	2.70
18	1.50±0.70	12.20±7.00	0.50	3.00
20	5.20±0.80	no bead	3.80	6.40

4.2 Butyl Rubber Content in Electrospinning of Polystyrene/Butyl Rubber Blends

As mentioned previously, 20 wt% polystyrene concentration was needed for making fibers without beads, and four different wt% butyl rubber concentrations, namely 20 wt%, 18 wt%, 15 wt%, and 10 wt% were used in the electrospinning of the blends. The polystyrene and butyl rubber blends were prepared by using volume ratios. Electrospinnable blend solutions which contain higher weight concentrations of butyl rubber were prepared by using 10 wt% BR solutions rather than 20 wt% BR solutions. This is because 20 wt% BR solutions have higher viscosity values than 10 wt% BR solutions. That means the amount of butyl rubber in the electrospinnable blend solutions can be increased by using its

low percentage solution. Such an increase provides the means to increase butyl rubber by volume ratio in the overall solution.

Figure 4.3 shows the percentages of butyl rubber in the total polymer blends, which are suitable for electrospinning. The total polymer concentration was varied from 16.7 to 9.8 wt% in the solution and the butyl rubber concentration was changed from 10 to 80 wt%. The last point of each curve in **Figure 4.3** denotes the maximum butyl rubber content beyond which the blend is not suitable for electrospinning.

We used different butyl rubber solutions with concentrations decreasing from 20 to 10 wt% in THF. By using 10 wt% BR solutions rather than 20 wt% BR solutions, electrospinning of blends containing higher amount of butyl rubber was managed. In **Figure 4.4**, SEM images of PS/BR blends that were not successfully electrospun are given. These images were taken from the points where the maximum amount of butyl rubber content could be electrospun including butyl rubber solutions prepared with different concentrations. The blend solutions were electrospun at 20 kV applied voltage, 10 cm tip-to-collector distance, and 0.1 ml/min solution flowrate adjusted by the syringe pump.

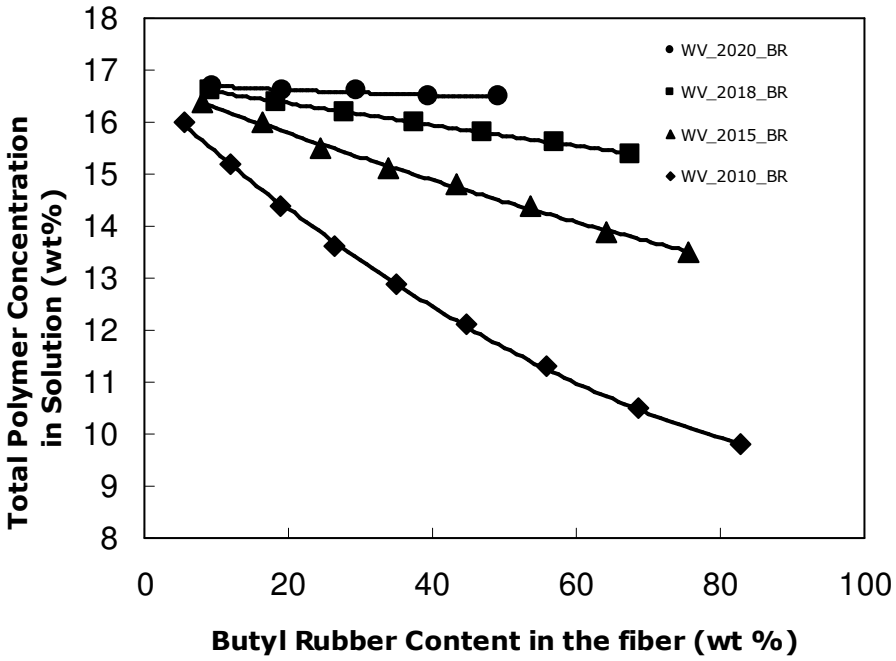

Figure 4.3 Butyl rubber fiber content (wt%) in the total polymer concentration in solution.

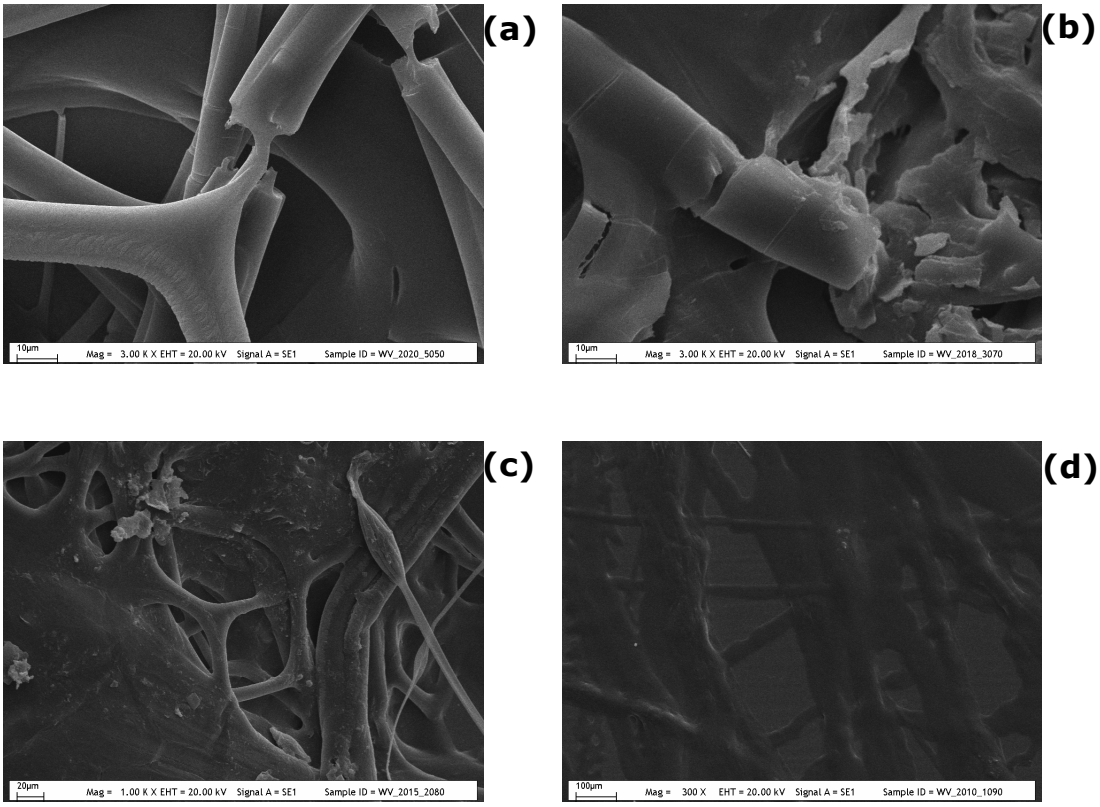

Figure 4.4 SEM images of polystyrene/butyl rubber blends (WV-20/20-50/50, WV-20/18-30/70, WV-20/15-20/80, and WV-20/10-10/90) electrospun at 10 cm tip-to-collector distance, 20 kV applied voltage, and 0.1 ml/min solution flowrate containing **(a)** 49.1; **(b)** 67.5; **(c)** 75.6; **(d)** 82.7 wt% butyl rubber in the fibers.

Some interesting fibers having different morphologies were also observed. These are fibers with porous structure, fibers having flat ribbon shape, branched fibers, fibers with junctions, split fibers, and some discontinuous fibers. SEM micrographs of these samples are shown in **Figure 4.5**.

In addition to fibers having interesting morphologies, some fibers having sub-micron diameters were also observed and illustrated in **Figure 4.6**.

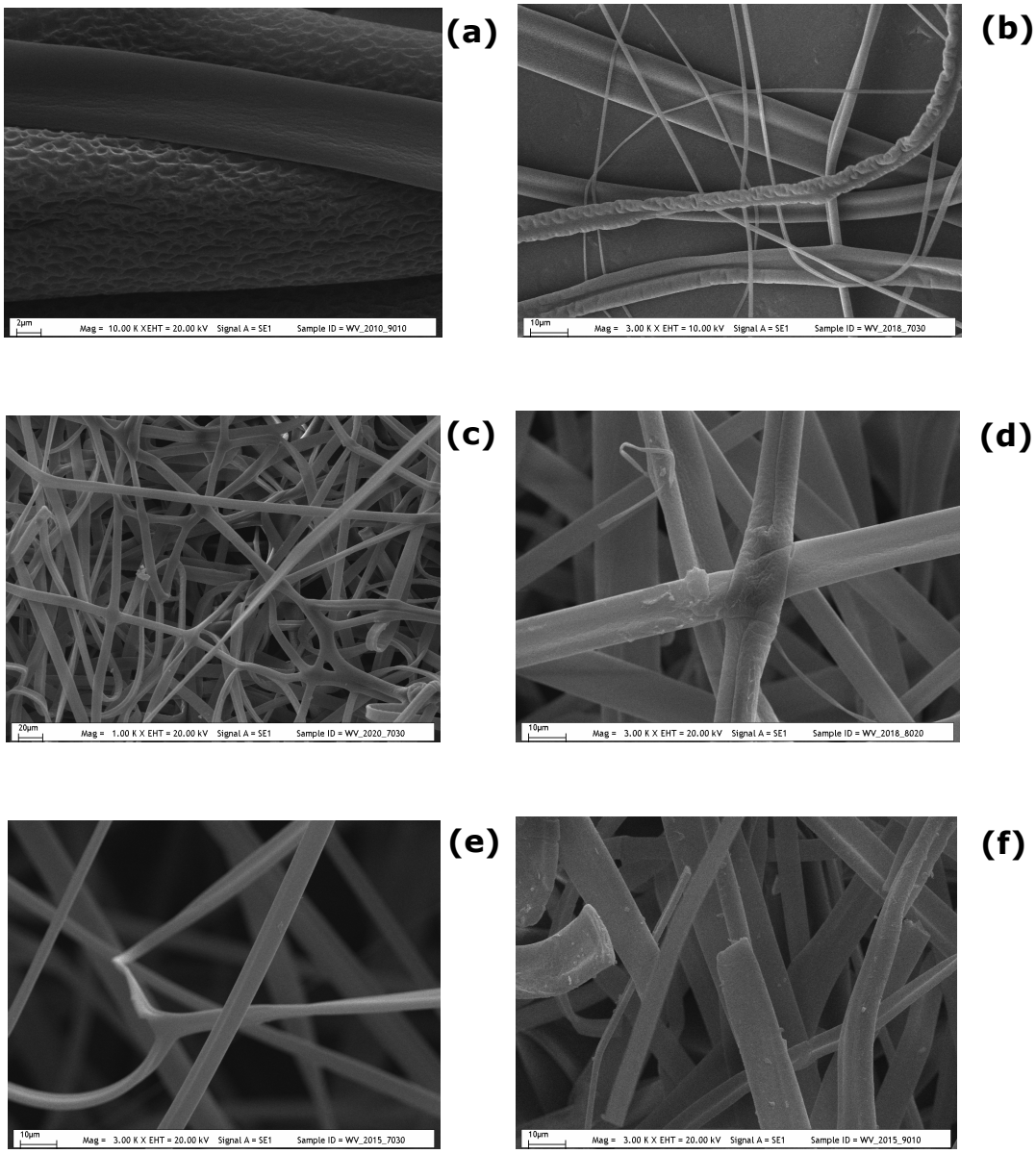

Figure 4.5 SEM images of polystyrene/butyl rubber blends at 10 cm, 20 kV **(a)** 0.1 ml/min containing 5.6 wt% butyl rubber (WV-20/10-90/10); **(b)** 0.05 ml/min containing 27.8 wt% butyl rubber (WV-20/18-70/30); **(c)** 0.1 ml/min containing 29.5 wt% butyl rubber (WV-20/20-70/30); **(d)** 0.1 ml/min containing 18.3 wt% butyl rubber (WV-20/18-80/20); **(e)** 0.1 ml/min containing 24.5 wt% butyl rubber (WV-20/15-70/30); **(f)** 0.1 ml/min containing 7.9 wt% butyl rubber (WV-20/15-90/10).

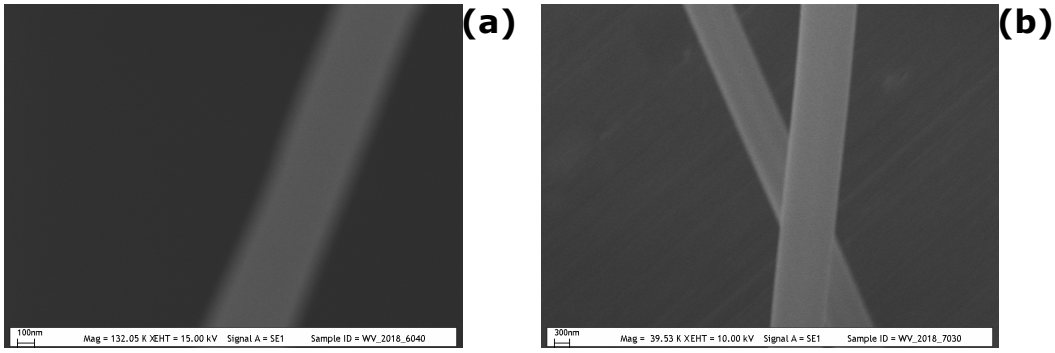

Figure 4.6 SEM images of polystyrene/butyl rubber blends at 10 cm, 10 kV, and 0.1 ml/min containing **(a)** 37.5 w % butyl rubber (WV-20/18-60/40) ;**(b)** 27.8 wt% butyl rubber (WV-20/18-70/30)

4.2.1 Effects of Applied Voltage

The first parametric study done was to investigate the effect of electrostatic voltage on the formation of polystyrene/butyl rubber fibers. **Figure 4.7** illustrates SEM images of electrospun fibers at low butyl rubber content. The distance and flowrate of the polymer solution were set to 10 cm, and 0.1 ml/min, respectively. The applied electrical voltage was set as 10 kV, 15 kV, and 20 kV. The average fiber diameters were found to decrease when the applied voltage increased from 10 to 20 kV. The average fiber diameters are given in **Table 4.2**.

The same tendency was observed at higher % butyl rubber content in the fibers. SEM images and average fiber diameters are given in **Figure 4.8** and **Table 4.3**, respectively. However, bead formation was observed at high butyl rubber content in the fibers.

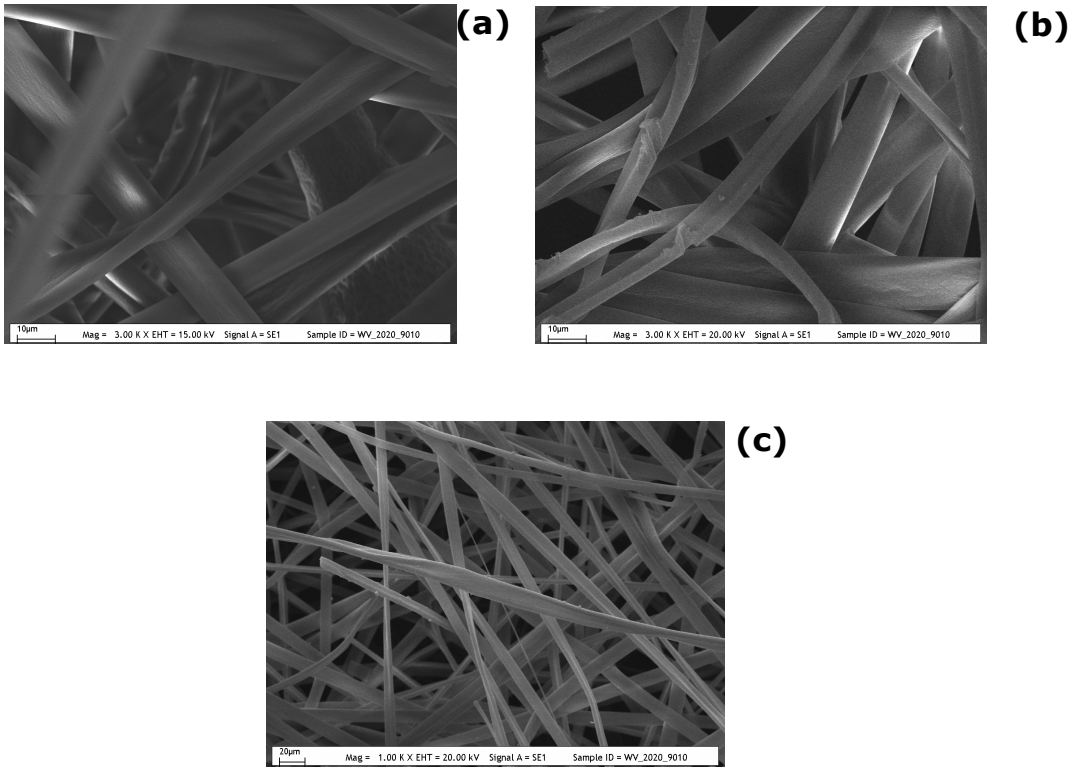

Figure 4.7 SEM images of polystyrene/butyl rubber blends (WV-20/20-90/10) containing 9.6 wt% butyl rubber fibers electrospun at 10 cm tip-to-collector distance, and three different applied voltages **(a)** 10 kV, **(b)** 15 kV, and **(c)** 20 kV.

Table 4.2 Average fiber diameters of polystyrene/butyl rubber blends containing 9.6 % butyl rubber fibers electrospun at 10, 15, and 20 kV applied voltages.

Applied Voltage (kV)	Average fiber diameter (µm)
10	9.80±4.50
15	7.30±3.60
20	6.50±2.90

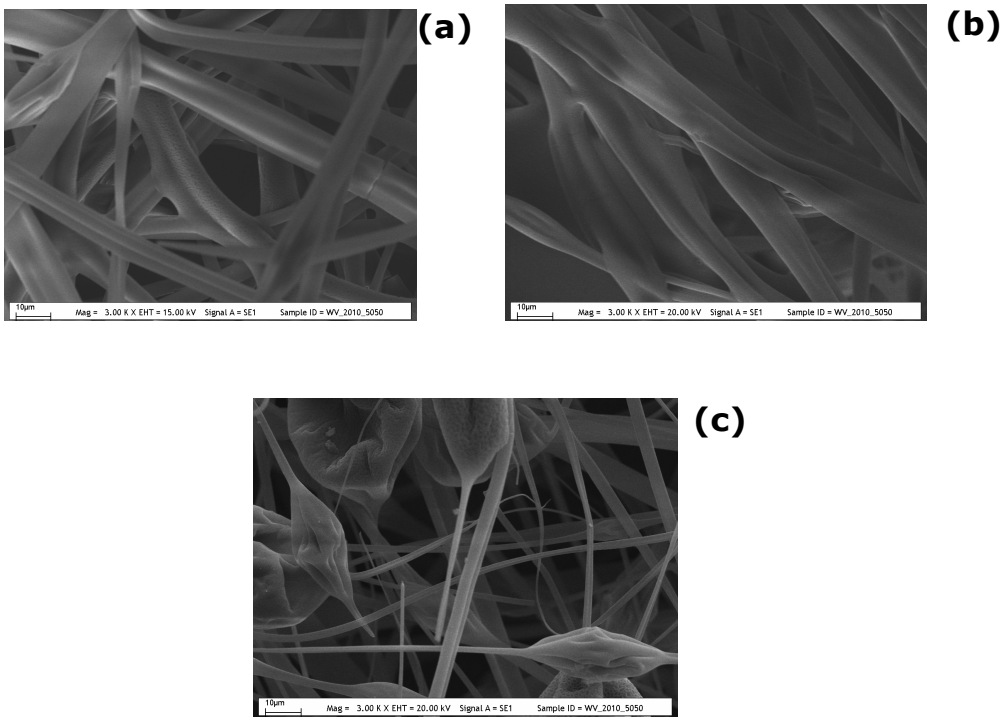

Figure 4.8 SEM images of polystyrene/butyl rubber blends (WV-20/10-50/50) containing 35 % butyl rubber fibers electrospun at 10 cm tip-to-collector distance, and three different applied voltages **(a)** 10 kV, **(b)** 15 kV, and **(c)** 20 kV.

Table 4.3 Average fiber diameters of polystyrene/butyl rubber blends containing 35 % butyl rubber fibers electrospun at 10, 15, and 20 kV applied voltages.

Applied Voltage (kV)	Average fiber diameter (µm)
10	5.00±3.10
15	4.70±2.50
20	2.60±2.10

4.2.2 Effects of Tip-to-Collector Distance

Figure 4.9 illustrates SEM images of electrospun fibers at various butyl rubber contents electrospun at different tip-to-collector distance. The applied voltage and flowrate of the polymer solution were set to 20 kV, and 0.1 ml/min, respectively. The tip-to-collector distance was increased from 7 cm to 15 cm. Average fiber diameters are given in **Table 4.4**. Tip-to-collector distance did not affect the average fiber diameter, but a significant decrease was observed for 29.5 % BR with 15 cm distance between tip and the collector. On the other hand, a distance of 7 cm was not enough for solvent evaporation, and fusion of some fibers was observed.

Table 4.4 Average fiber diameters of polystyrene/butyl rubber blends containing various (9.6, and 29.5 %) butyl rubber fibers electrospun at 7, 10, and 15 cm working distance.

Distance (cm)	Average fiber diameter (μm) (9.6 % BR)	Average fiber diameter (μm) (29.5 % BR)
7	6.50±3.80	6.50±2.20
10	6.50±2.90	6.50±2.10
15	6.50±3.40	2.90±1.90

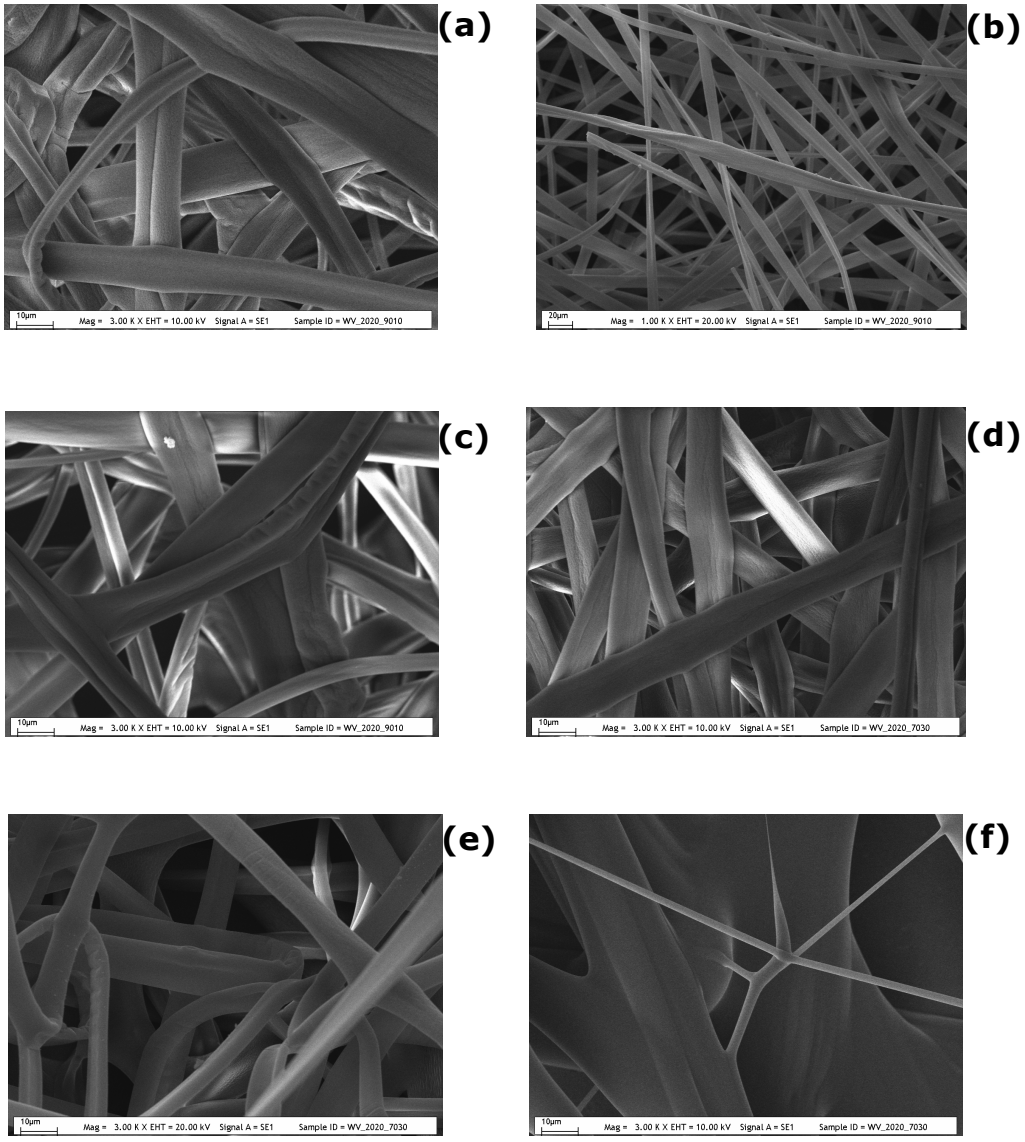

Figure 4.9 SEM images of polystyrene/butyl rubber blends (WV-20/20-90/10, WV-20/20-70/30) containing various (9.6, and 29.5 %) butyl rubber fibers electrospun at 20 kV applied voltage, and 0.1 ml/min and three different tip-to-collector distance **(a, d)** 7 cm, (**b, e)** 10 cm, and **(c, f)** 15 cm.

4.2.3 Effects of Solution Flowrate

Figure 4.10 and **4.11** illustrate SEM images of electrospun fibers containing 9.6, and 33.8 % butyl rubber. The applied voltage and tip-to-collector distance of the polymer solution were set to 20 kV, and 10 cm, respectively. The solution flowrate was increased from 0.05 ml/min to 0.1 ml/min. The average fiber diameters of electrospun blend solutions containing low BR content showed an increase with an increase in the flowrate from 0.05 ml/min to 0.08 ml/min but between 0.08 ml/min to 0.1 ml/min, they remained unchanged. On the other hand, average fiber diameters of electrospun blend solutions containing high BR content stayed almost same between 0.05 ml/min to 0.08 ml/min but flowrates between 0.08 ml/min to 0.1 ml/min, an increase was observed. Similar behaviour was also observed in the literature in the electrospinning of two chemically distinct thermoplastic elastomers based on block copolymers of styrene and isoprene [54]. The average fiber diameters are illustrated in **Table 4.5**.

Table 4.5 Average fiber diameters of polystyrene/butyl rubber blends containing various (9.6, and 33.8 %) butyl rubber fibers electrospun at the flowrates of 0.05, 0.08, and 0.1 ml/min.

Flowrate (ml/min)	Average fiber diameter (μm) (9.6 % BR)	Average fiber diameter (μm) (33.8 % BR)
0.05	4.70±1.80	5.60±2.60
0.08	6.50±2.00	5.60±2.30
0.10	6.50±2.90	7.00±2.10

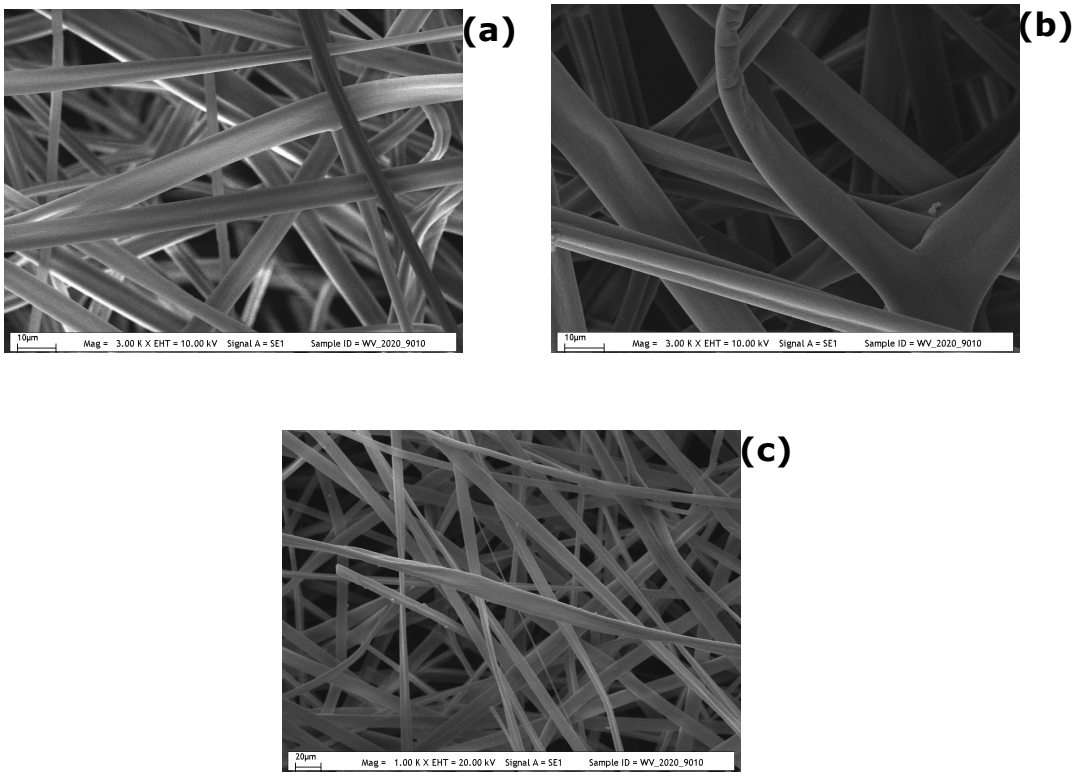

Figure 4.10 SEM images of polystyrene/butyl rubber blends (WV-20/20-90/10) containing 9.6 % butyl rubber fibers electrospun at 20 kV applied voltage and 10 cm, and three different solution flowrates **(a)** 0.05 ml/min, (**b)** 0.08 ml/min, and **(c)** 0.1 ml/min.

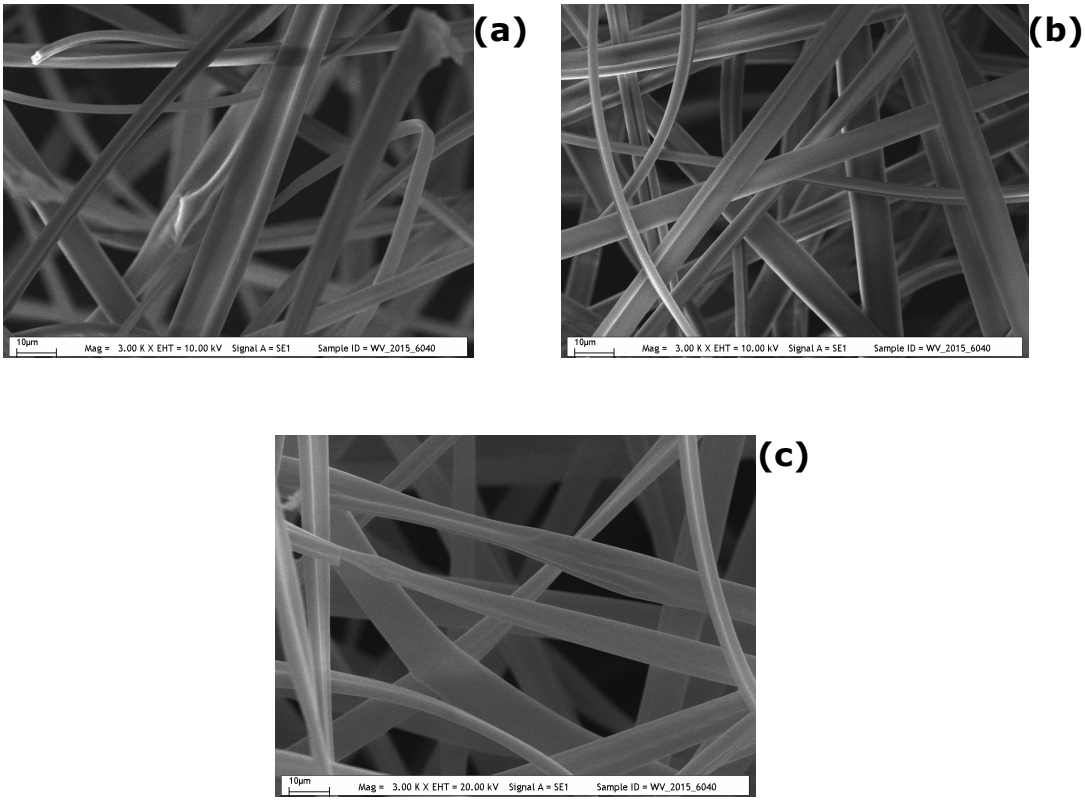

Figure 4.11 SEM images of polystyrene/butyl rubber blends (WV-20/15-60/40) containing 33.8 % butyl rubber fibers electrospun at 20 kV applied voltage, and 10 cm and three different solution flowrates **(a)** 0.05 ml/min, (**b)** 0.08 ml/min, and **(c)** 0.1 ml/min.

4.2.4 Effects of Butyl Rubber Content and Solution Viscosity

The viscosities various PS/BR blends are given in **Table 4.6**. The change of viscosity with BR content in the total polymer is given in **Figure 4.12**. The viscosity of the blend solutions increases with the increase of BR. This is because of the higher viscosity of BR solution than that of PS solution. The 20 wt% PS in THF has a

viscosity of 260 cP while 10 wt% BR in THF has a viscosity of 440 cP.

Table 4.6 Viscosities of PS/BR polymer blends in THF at 25°C

Composition (v/v)	Butyl rubber in blend (wt%)	Value (cP)
WV-20/20-90/10	9.6	413
WV-20/20-70/30	29.5	640
WV-20/20-50/50	49.0	867
WV-20/18-90/10	9.0	374
WV-20/18-70/30	27.8	480
WV-20/18-50/50	46.8	560
WV-20/18-30/70	67.5	1000
WV-20/15-90/10	7.9	320
WV-20/15-70/30	24.5	407
WV-20/15-50/50	43.2	450
WV-20/15-20/80	75.5	800
WV-20/10-90/10	5.6	267
WV-20/10-70/30	18.7	287
WV-20/10-40/60	44.6	327
WV-20/10-10/90	82.6	400

Figure 4.13 illustrates SEM images of electrospun fibers at various butyl rubber contents. The applied voltage, tip-to-collector distance, and flowrate of the polymer solution were set to 10 kV, 10 cm, and 0.1 ml/min, respectively. The BR content in the fiber was increased from 9.6 to 68.6 %. The average fiber diameters are given in **Table 4.7**. The average fiber diameters were found to decrease when the amount of butyl rubber increased in the PS/BR

blend solutions. Some beads formed at higher BR contents. Bead formation was observed first in **Figure 4.13 (d)**. The BR content was 33.8 % in **Figure 4.13 (d)**, and further increase in BR resulted in more beads. Moreover, the average fiber diameter was found below 1 μm.

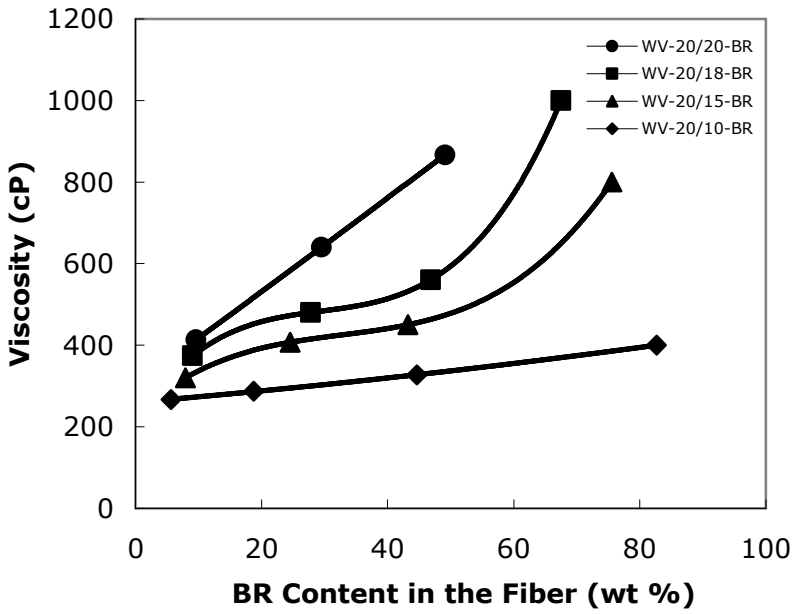

Figure 4.12 The change of viscosity of blend solution with BR content in fiber.

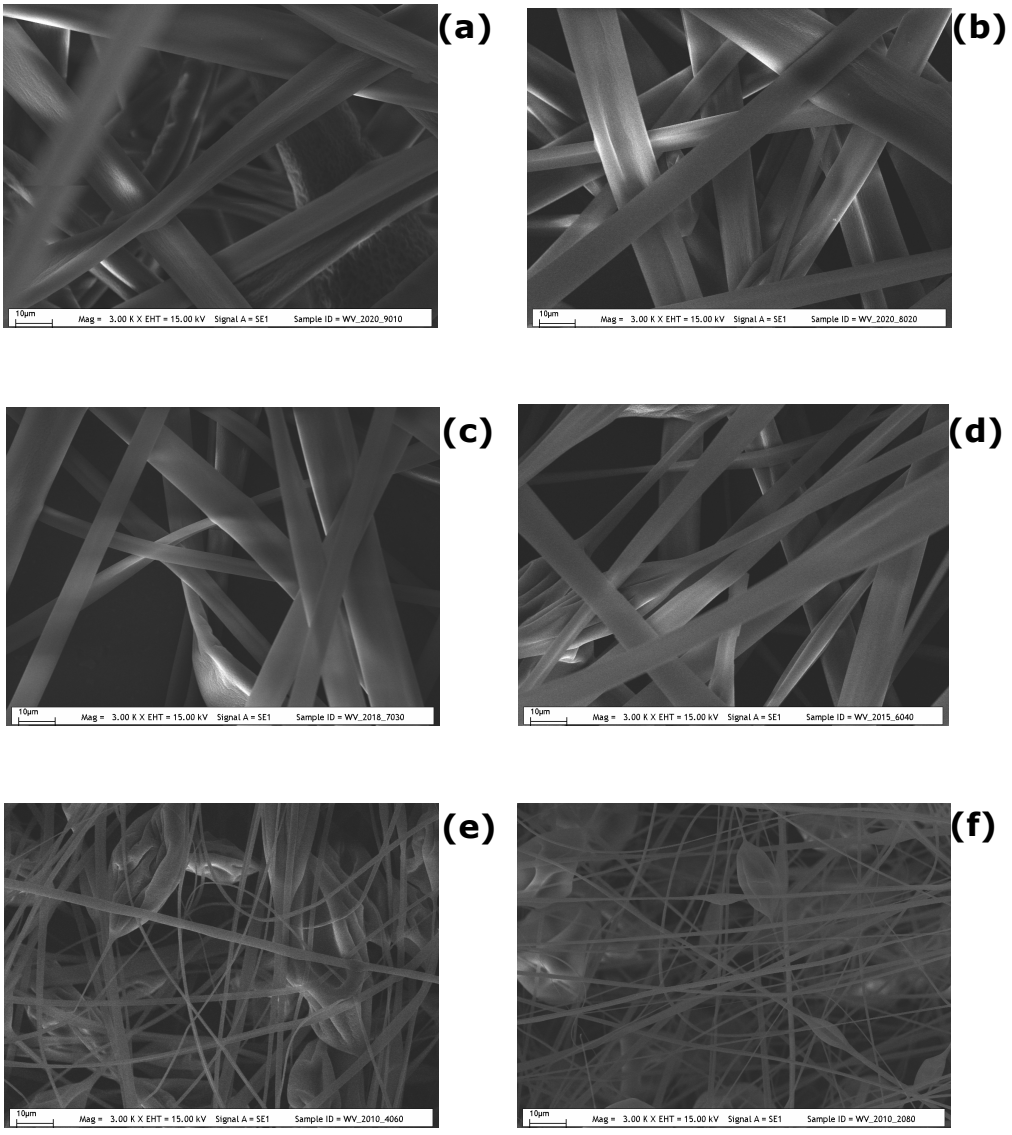

Figure 4.13 SEM images of polystyrene/butyl rubber blends containing **(a)** 9.6 %, **(b)** 19.3 %, **(c)** 27.8 %, **(d)** 33.8 %, **(e)** 44.6 %, and **(f)** 68.6 % butyl rubber fibers electrospun at 10 kV applied voltage, 10 cm tip-to-collector distance, and solution flowrate of 0.1 ml/min.

Table 4.7 Average fiber diameters of polystyrene/butyl rubber blends containing 9.6, 19.3, 27.8, 33.8, 44.6, and 68.6 % BR electrospun at 10 kV applied voltage, 10 cm tip-to-collector distance, and solution flowrate of 0.1 ml/min.

Butyl rubber (wt%)	Average fiber diameter (μm)
9.6	9.80±4.50
19.3	8.00±4.50
27.8	7.20±3.90
33.8	4.20±2.90
44.6	1.20±0.60
68.6	0.76±0.50

4.2.5 Effect of Non-ionic Surfactant Addition

A non-ionic surfactant, Triton-X 405 was added to the PS/BR blends with the aim to obtain fibers with smaller diameters. The addition of non-ionic surfactant increased the conductivity of solution about thirty times. The conductivity values of PS/BR blends are listed in **Table 4.8**. The conductivity of the solution with Triton-X 405 is given as the last figure in the last column of **Table 4.8**.

Table 4.8 Conductivities of PS/BR polymer blends in THF at 25°C

Composition (v/v)	Butyl rubber in blend (wt%)	Conductivity (μS/cm)
WV-20/20-90/10	9.6	0.004
WV-20/20-70/30	29.5	0.006
WV-20/20-50/50	49.0	0.005
WV-20/18-90/10	9.0	0.005
WV-20/18-70/30	27.8	0.005
WV-20/18-50/50	46.8	0.006
WV-20/18-30/70	67.5	0.011
WV-20/15-90/10	7.9	0.004
WV-20/15-70/30	24.5	0.006
WV-20/15-50/50	43.2	0.008
WV-20/15-20/80	75.5	0.007
WV-20/10-90/10	5.6	0.006
WV-20/10-70/30	18.7	0.006
WV-20/10-40/60	44.6	0.006
WV-20/10-10/90	82.6	0.005
WV-20/15-70/30 with 1 v % Triton-X 405	24.5	0.168

The SEM images of electrospun fibers containing 24.5 % butyl rubber contents are given in **Figure 4.14**. The applied voltage, and tip-to-collector distance were set to 20 kV, and 10 cm, respectively. The solution flowrate was set to 0.1 ml/min. The addition of 1 v % of Triton-X 405 caused a decrease in the average fiber diameter. Also, fibers were distributed more uniform in the

collector. The average fiber diameter of electrospun fibers with the addition of Triton-X 405 is shown in **Table 4.9**.

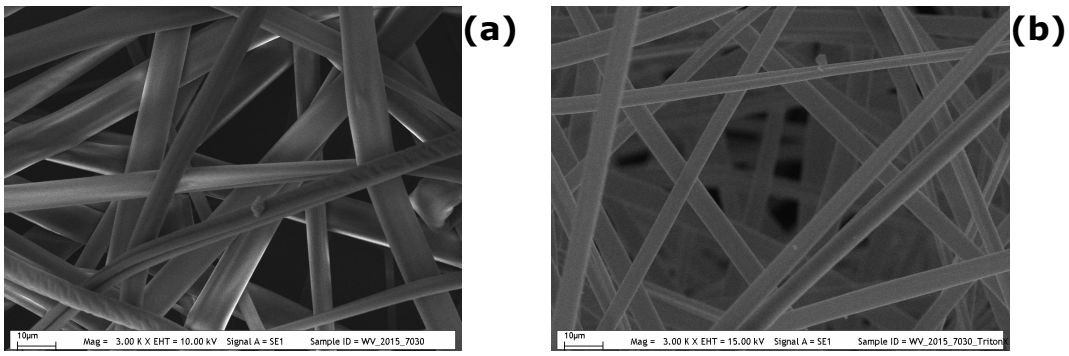

Figure 4.14 SEM images of PS/BR blends containing **(a)** 0 % , **(b)** 1 % of Triton-X 405. Other values: BR: 24.5, voltage: 20 kV, tip-to-collector distance: 15 cm and solution flowrate: 0.1 ml/min.

Table 4.9 The average fiber diameters of PS/BR blends containing 24.5 % butyl rubber fibers with 1 % of Triton-X 405.

Butyl rubber (wt%)	**Average fiber diameter (µm) (0 v % Triton-X 405)**	**Average fiber diameter (µm) (1 v % Triton-X 405)**
24.5	5.30±2.30	4.70±1.00

4.2.6 Effect of Sodium Sulphate (Na_2SO_4), Potassium Hydroxide (KOH), and Copper (II) Chloride ($CuCl_2$) Addition

The effect of the addition of Na_2SO_4, KOH, and $CuCl_2$ at 1 % to PS/BR blend solutions was illustrated in **Figure 4.15**. The average fiber diameters are given in **Table 4.10**. The addition of Na_2SO_4, and KOH did not change the diameter significantly but a small increase was observed in the case of $CuCl_2$ addition. The addition of Na_2SO_4 eliminated the low level bead formation in the same specimen.

Table 4.10 The average fiber diameters of PS/BR blends.

Butyl rubber (wt%)	**Average fiber diameter (μm)**
18.7	7.70±2.80
18.7 with 1 wt% Na_2SO_4	7.10±3.20
27.8	7.50±4.70
27.8 % with 1 wt% KOH	7.40±2.10
9.6	6.50±3.20
9.6 % with 1 wt% $CuCl_2$	7.50±3.40

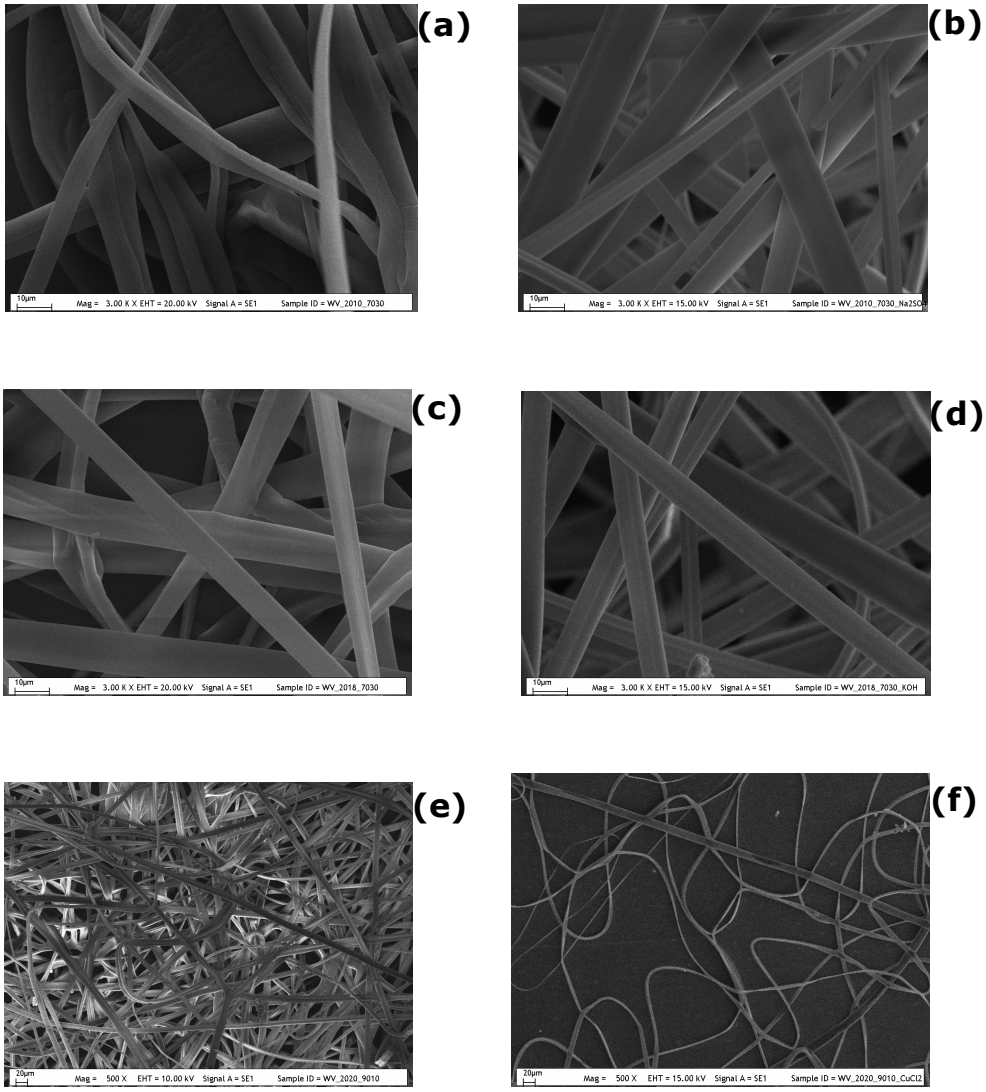

Figure 4.15 SEM images of PS/BR blends containing **(a)** BR: 18.7 %, **(b)** BR: 18.7 % with 1 wt% Na_2SO_4, **(c)** BR: 27.8 %, **(d)** BR: 27.8 % with 1 wt% KOH, **(e)** BR: 9.6 %, and **(f)** BR: 9.6 % with 1 wt% $CuCl_2$. Voltage: 20 kV, tip-to-collector distance: 10 cm, and solution flowrate: 0.1 ml/min.

CHAPTER 5

CONCLUSIONS

1. Polystyrene/butyl rubber fibers, with average diameters from 760 nm to around 10 μm were produced.

2. The increase in the applied electrical voltage decreased the average fiber diameter.

3. No significant change in the average fiber diameters was observed when the tip-to-collector distance was changed.

4. The increase in the solution flowrate caused an increase in the average fiber diameter.

5. The increase in the butyl rubber content in the blends decreased the average fiber diameter, but beads formed at high butyl rubber contents.

6. The addition of small amounts of non-ionic surfactant to the PS/BR blends caused a small decrease in the average fiber diameter.

7. The addition of Na_2SO_4, and KOH did not change the average fiber diameter significantly but a small increase was observed in the case of $CuCl_2$ addition.

8. The increase BR content in the blend yielded with an increase in the viscosity of blend solution.

9. The optimum conditions for electrospinning of PS/BR blends were found out as 20 kV of applied voltage, 0.05 ml/min of flowrate, and both 10 cm and 15 cm of tip-to-collector-distance.

CHAPTER 6

RECOMMENDATIONS

- Different types of anionic or cationic surfactants should be tried in order to obtain PS/BR fibers with smaller diameter.

- Mechanical characterization of the electrospun blends need to be done to find out the mechanical properties of PS/BR blend fibers.

REFERENCES

1. Ko, F. K., '*Bridging the Gap between Nano and Macro World*', Drexel Uni, Philadelphia, Pa.

2. Huang, Z. M., Zhang, Y. Z., Kotaki, M., Ramakrishna, S., '*A review on polymer nanofibers by electrospinning and their applications in nanocomposites*', Comp. Sci. & Tech., 2003, 63, 2223-2253.

3. Ondarcuhu, T., Joachim, C., *´Drawing a single nanofibre over hundreds of microns´*, Europhys. Lett., 42, 215-220.

4. Harfenist, S. A., Cambron, S. D., Nelson, E. W., Berry, S. M., Isham, A. W., Crain M. M., Walsh K. M., Keynton, R. S., and Cohn, R. W., *´Direct Drawing of Suspended Filamentary Micro- and Nanostructures from Liquid Polymers´*, Nanoletters, Vol. 4, 1931-1937.

5. Schönenberger, C., van der Zande, B. M. I., Fokkink, L. G. J., Henny, M., Schmid, C., Krüger, M., Bachtold, A., Huber, R., Birk, H., and Staufer, U., *´Template Synthesis of Nanowires in Porous Polycabonate Membranes: Electrochemistry and Morphology´*, J. Phys. Chem., 1997, 101, 5497-5505.

6. Feng, L., Li, S., Li, H., Zhai, J., Song, Y., Jiang, L., and Zhu, D., *´SuperHydrophobic Surface of Aligned Polyacrylonitrile Nanofibers´*, Angew. Chem. Int. Ed., 2002, 41, No.7.

7. Martin, C. R., *´Template Synthesis of Electronically Conductive Polymer Nanostructures´*, Acc. Chem. Res., 1995, 28, 61-68.

8. Martin, C. R., *´Membrane-Based Synthesis of Nanomaterials´*, Chem. Mater., 1996, 8, 1739-1746.

9. Huczko, A., *´Template-based synthesis of nanomaterials´*, Appl. Phys., A 70, 365-376 (2000).

10. Ma, P. X., Zhang, R., *´Synthetic nano-scale fibrous extracellular matrix´*, J. Biomed. Mater. Res., 1999, 46(1), 60-72.

11. Lo, H., Kadiyala, S., Guggino, S. E., and Leong, K. W., *´Poly(L-lactic acid) foams with cell seeding and controlled-release capacity´*, J. Biomed. Mater. Res., 1996, 30(4), 475-484.

12. Zhang, R., Ma, P. X., *´Poly (α-hydroxyl acids)/hydroxyapatite porous composites for bone-tissue engineering. I. Preparation and morphology´*, J. Biomed. Mater. Res., 1999, 44(1), 446-455.

13. Ramakrishna, S., Fujihara, K., Teo, W. E., Lim, T. C., Ma, Z., *´An Introduction to Electrospinning and Nanofibers´*, World Scientific Publishing, Singapore.

14. Hartgerink, J. D., Beniash, E., Stupp, S. I., *´Self-Assembly and Mineralization of Peptide-Amphiphile Nanofibers´*, Science, 2001, 294, 1684-1687.

15. Niece, K. L., Hartgerink, J. D., Donners, J. J. J. M., and Stupp, S. I., *´Self-Assembly Combining Two Bioactive Peptide-Amphiphile Molecules into Nanofibers by Electrostatic Attraction´*, J. Am. Chem. Soc., 2003, 125, 7146-7147.

16. Zhang, S., Gelain, F., Zhao, X., *´Designer Self-assembling peptide nanofiber scaffolds for 3D tissue cell cultures´*, Seminars in Can. Biol. 15, 2005, 413-420.

17. de Moel, K., Alberda van Ekkenstein, G. O. R., Nijland, H., Polushkin, E., and ten Brinke, G., *´Polymeric Nanofibers Prepared from Self-Organized Supramolecules´*, Chem. Mater., 2001, 13, 4580-4583.

18. Formhals, A., *´Process and apparatus for preparing artificial threads´*, US Patents, 1934, 1,975,504.

19. Vonnegut, B., Neubauer, R. L., *´Production of monodisperse liquid particles by electrical atomization´*, J. of Colloid Science, 1952, 7, 616.

20. Taylor, G. I., *´Electrically Driven Jets´*, Proc. of Roy. Soc. of London, 1969, 313, 453-475.

21. Baumgarten, P., *´Electrostatic spinning of Acrylic microfibers´*, J. Colloid Interface Science, 1971, 36, 71.

22. Fang, X., Reneker, D. H., *´DNA fibers by Electrospinning´*, J. Macromol. Sci. Phys., 1997, B36(2), 169-173.

23. Shin, Y. M., Hohman, M. M., Brenner, M. P., Rutledge, G. C., *´Experimental characterization of electrospinning: the electrically forced jet and instabilities´*, Polymer, 2001, 42, 9955-9967-

24. Yang, F., Murugan, R., Wang, S., Ramakrishna, S., *´Electrospinning of nano/micro scale poly (L-lactic acid) aligned fibers and their potential in neural tissue engineering´*, Biomater., 2005, 26, 2603-2610.

25. Fong, H., Chun, I., Reneker, D. H., *´Beaded nanofibers formed during electrospinning´*, Polymer, 1999, 40, 4585-4592.

26. Reneker, D. H., Chun, I., *´Nanometre diameter fibres of polymer, produced by electrospinning´*, Nanotechnology, 1996, 7, 216-223.

27. Shin, Y. M., Hohman, M. M., Brenner, M. P., Rutledge, G. C., *´Electrospinning: A whipping fluid jet generates submicron polymer fibers´*, Appl. Phys. Let., 2001, V78, No.8, 1149-1151.

28. Doshi, J., Reneker, D. H., *´Electrospinning and Applications of Electrospun Fibers´*, Indus. Appl. Soc. Ann. Meet., 1993, V.3, 1698-1703.

29. Subbiah, T., Bhat, G. S., Tock, R. W., Parameswaran, S., Ramkumar, J. S., *´Electrospinning of Nanofibers´*, J. of Appl. Poly. Sci., 2005, V.96, 557-569.

30. McCann, J. T., Li, D., Xia, Y., *´Electrospinning of nanofibers with core-sheath, hollow, or porous structures´*, J. of Mater. Chem., 2005, 15, 735-738.

31. Koombhongse, S., Liu, W., Reneker, D. H., *´Flat ribbons and other shapes by electrospinning´*, J. of Poly. Sci. Poly. Phys. Ed., 2001, 39, 2598-2606.

32. Diaz de Leon, M. J., *´Electrospinning Nanofibers of Polyaniline and Polyaniline/(Polystyrene and Polyethylene Oxide) Blends´*, Proc. of Nat. Con. Undergrad. Res., 2001, Lexington, Uni. of Kentucky.

33. Frenot, A., Chronakis, I. S., *´Polymer nanofibers assembled by electrospinning´*, Cur. Opi. in Col. and Inter. Sci., 2003, 8, 64-75.

34. Reneker, D. H., Yarin, A. L., Fong, H., and Koombhongse, S., *´Bending instability of electrically charged liquid jets of polymer solutions in electrospinning´*, J. of Appl. Phys., 2000, V.87, No.9, 4531-4547.

35. Rutledge, G. C., Shin, M. Y., Warner, S. B., Buer, A., Grimler, M., Ugbolue, M., *'Investigation of the Formation and Properties Electrospun Fibers'*, National Textile Center Annual Report, November 2000.

36. Tan, E. P. S., Ng, S. Y., Lim, C. T., '*Tensile testing of a single ultrafine polymeric fiber*', Biomaterials, 2005, 26, 1453-1456.

37. Wannatong, L., Sirivat, A., and Supaphol, P., '*Effects of solvents on electrospun polymeric fibers: preliminary study on polystyrene'*, Polym. Int., 2004, 53, 1851-1859.

38. Jarusuwannapoom, T., Hangrojjanawiwat, W., Jitjaicham, S., Wannatong, L., Nithitanakul, M., Pattamaprom, C., Koombhongse, P., Rangkupan, R., Supaphol, P., '*Effect of solvents on electrospinnability of polystyrene solutions and morphological appearance of resulting electrospun polystyrene fibers*', European Poly. J., 2005, 41, 409-421.

39. Mit-uppatham, C., Nithitanakul, M., Supaphol, P., '*Ultrafine Electrospun Polyamide-6 Fibers: Effect of Solution Conditions on Morphology and Average Fiber Diameter*', Macromol. Chem. Phys., 2004, 205, 2327-2338.

40. Choi, J. S., Lee, S. W., Jeong, L., Bae S. H., Min, B. C., Youk, J. H., Park, W. H., '*Effect of organosoluble salts on the nanofibrous structure of electrospun poly(3-hydroxybutyrate-co-3-hydroxyvalerate)*', Int. J. of Bio. Macro.,2004, 34, 249-256.

41. Son, W. K., Youk, J. H., Lee, T. S., Park, W. H., '*The effects of solution properties and polyelectrolyte on electrospinning of ultrafine ply(ethylene oxide) fibers*', Polymer, 2004, 45, 2959-2966.

42. Lin, T., Wang, H., Wang, H., Wang, X., '*The charge effect of cationic surfactants on the elimination of fibre beads in the electrospinning of polystyrene*', Nanotechnology, 2004, 15, 1375-1381.

43. Yang, Q., Li, Z., Hong, Y., '*Influence of Solvents on the Formation of Ultrathin Uniform Poly(vinyl pyrrolidone) Nanofibers with Electrospinning*', J. of Poly. Sci.:Part B:Poly. Phys., 2004, V.42, 3721-3726.

44. Zeng, J., Xu, X., Chen, X., Liang, Q., Bian, X., Yang, L., Jing, X., '*Biodegradable electrospun fibers for drug delivery*', J. of Cont. Rel., 2003, 92, 227-231.

45. Drew, C., Wang, X., Samuelson, L. A., and Kumar, J., '*The Effect of Viscosity and Filler on Electrospun Fiber Morphology*', J. of Macro. Sci., 2003, V.A40, 12, 1415-1422.

46. Shenoy, S. L., Bates, D. W., Frisch, H. L., Wnek, G. E., '*Role of chain entanglements on fiber formation during electrospinning of polymer solutions: good solvents, non-specific polymer-polymer interaction limit*', Polymer, 2005, 46, 3372-3384.

47. Koski, A., Yim, K., Shivkumar, S., '*Effect of molecular weight on fibrous PVA produced by electrospinning'*, Mater. Let., 2004, 58, 493-497.

48. Megelski, S., Stephens, J. S., Chase, D. B., and Robalt, J. F., '*Micro- and Nanostructured Surface Morphology on Electrospun Polymer Fibers*', Macromolecules, 2002, 35, 8456-8466.

49. Zheng, J., He, A., Li, J., Xu, J., Han, C. C., '*Studies on the controlled morphology and wettability of polystyrene surfaces by electrospinning or electrospraying*', Polymer, 2006, 47, 7095-7102.

50. Matthews, J. A., Wnek, G. E., Simpson, D. G., and Bowlin, G. L., '*Electrospinning of Collagen Nanofibers*', Biomacromolecules, 2002, 3, 232-238.

51. Lee, K. H., Kim, H. Y., Bang, H. J., Jung, Y. H., Lee, S. G., '*The change of bead morphology formed on electrospun polystyrene fibers*', Polymer, 2003, 44, 4028-4034.

52. Wang, C., Hsu, C. H., and Lin, J. H., '*Scaling Laws in Electrospinning of Polystyrene Solutions'*, Macromolecules, 2006, 39, 7662-7672.

53. Baker, S. C., Atkin, N., Gunning, P. A., Granville, N., Wilson, K., Wilson, D., Southgate, J., '*Characterisation of electrospun polystyrene scaffolds for three-dimensional in vitro biological studies*', Biomaterials, 2006, 27, 3136-6146.

54. Chuangchote, S., Sirivat, A., and Supaphol, P., '*Electrospinning of Styrene-Isoprene Copolymeric Thermoplastic Elastomers*', Poly. J., 2006, V.38, 9, 961-969.

55. Deitzel, J. M., Kleinmeyer, J., Harris, D., Beck Tan, N. C., '*The effect of processing variables on the morphology of electrospun nanofibers and textiles*', Polymer, 2001, 42, 261-272.

56. Zeng, J., Chen, X., Xu, X., Liang, Q., Bian, X., Yang, L., Jing, X., '*Ultrafine fibers Electrospun from Biodegradable Polymers*', J. of Appl. Poly. Sci., 2003, V.89, 1085-1092.

57. Casper, C. L., Stephens, J. S., Tassi, N. G., Chase, D. B., and, Rabolt, J. F., '*Controlling Surface Morphology of Electrospun Polystyrene Fibers: Effect of Humidity and Molecular Weight in the Electrospinning Process*',Macromolecules, 2004, 37, 573-578.

58. Gupta, P., Elkins, C., Long, T. E., Wilkes, G. L., '*Electrospinning of linear homopolymers of poly(methyl methacrylate): exploring relationships between fiber formation, viscosity, molecular weight and concentration in a good solvent'*, Polymer, 2005, 46, 4799-4810.

59. Lee, K. H., Kim, H. Y., Khil, M. S., Ra, Y. M., Lee, D. R., '*Characterization of nano-structured poly (ε-caprolactone) nonwoven mats via electrospinning'*, Polymer, 2003, 44, 1287-1294.

60. Deitzel, J., Beck Tan, N. C., Kleinmeyer, J. D., Rehrmann, J., Tevault, D., Reneker, D., Sendijarevic, I., McHugh, A '*Generation of Polymer Nanofibers Through Electrospinning*', ARL-TR-1989, 1999.

61. Greiner, A., Wendorff, J. H., '*Electrospinning: A Fascinating Method for the Preparation of Ultrathin Fibers*', Angew. Chem. Int. Ed., 2007, 46, 5670-5703.

62. Sun, D., Chang, C., Li, S., Lin, L., '*Near-Field Electrospinning*', Nanoletters, 2006, V.6, 4, 839-842.

63. Ebewele, R. O., '*Polymer Science & Technology*', CRC Press, Boca Raton, 1996.

64. Kang, M., Jung, R., Kim, H. S., Jin, H. J., '*Preparation of superhydrophobic polystyrene membranes by electrospinning*', Colloids and Surfaces A: Physicochem. Eng. Aspects, 2007.

65. Eda, G., Liu, J., Shivkumar, S., '*Solvent effects on jet evolution during electrospinning of semi-dilute polystyrene solutions*', Euro. Poly. J., 2007, 43, 1154-1167.

66. Miyauchi, Y., Ding, B., and Shiratori, S., '*Fabrication of a silver-ragwort-leaf-like super-hydrophobic micro/nanoporous fibrous mat surface by electrospinning*', Nanotechnology, 2006, 17, 5151-5156.

67. Eda, G., Liu, J., Shivkumar, S., '*Flight path of electrospun polystyrene solutions: Effects of molecular weight and concentration*', Mater. Let., 2007, 61, 1451-1455.

68. Shin, C., Chase, G. G., '*Nanofibers from recycle waste expanded polystyrene using natural solvent*', Poly. Bulletin, 2005, 55, 209-215.

69. Shin, C., '*A New Recycling Method for Expanded Polystyrene*', Packag. Technol. Sci., 2005, 18, 331-335.

70. Pattamaprom, C., Hongrojjanawiwat, W., Koombhongse, P., Supaphol, P., Jarusuwannapoo, T., Rangkupan, R., '*The Influence of Solvent Properties and Functionality on the Electrospinnability of Polystyrene Nanofibers*', Macromol. Mater. Eng., 2006, 291, 840-847.

71. Eda, G., Shivkumar, S., '*Bead structure variations during electrospinning of polystyrene'*, J. Mater. Sci., 2006, 41, 5704-5708.

72. Retrieved of December 31, 2007 from the World Wide Web: *http://www.azom.com/details.asp?ArticleID=1549*, Butyl Rubber-Polyisobutylene.

73. Viriyabanthorn, N., Mead, J. L., Stacer, R. G., Sung, G., '*Effect of carbon black loading on electrospun butyl rubber nonwoven mats*', Poly. Preprints, 2003, V.44, 2, 136-137.

74. Threepopnatkul, P., Murphy, D., Mead, J., '*Effects of Carbon Black Type on Breathable Butyl Rubber Membranes*', 25th ACS, 2006, Orlando, FL.

75. Kalra, V., Kakad, P. A., Mendez, S., Ivannikov, T., Kamperman, M., and Joo, Y. L., '*Self-Assembled Structures in Electrospun Poly(styrene-block-isoprene) Fibers*', Macromolecules, 2006, 39, 5453-5457.

76. Chuangchote, S., Sirivat, A., Supaphol, P., *'Electrospinning of Styrene-Isoprene Copolymeric Thermoplastic Elastomers'*, Poly. J.,2006, 38, 9, 961-969.

77. Ji, Y., Li, B., Ge, S., Sokolov, J. C., and Rafailovich, M. H., '*Structure and Nanomechanical Characterization of Electrospun PS/Clay Nanocomposite Fibers'*, Langmuir, 2006, 22, 1321-1328.

78. Wei, M., Lee, J., Kang, B., Mead, J., '*Preparation of Core-Sheath Nanofibers from Conducting Polymer Blends'*, Macromol. Rapid Commun., 2005, 26, 1127-1132.

79. Pan, C., Sun, C., Wei, H. M., Han, G. Z., Zhang, J. Z., Fujishima, A., Gu, Z. Z., '*Bio-inspired titanium dioxide film with extremely stable sper-amphilicity'*, Mater. Res. Bul., 2007, 42, 1395-1401.

80. Wutticharoenmongkol, P., Supaphol, P., Srikhirin, T., Kerdcharoen, T., Osotchan, T., *'Electrospinning of Polystyrene/poly(2-methoxy-5-(2'-ethyloxy)-1,4-phenylene vinylene) Blends'*, J. of Poly. Sci., 2005, 43, 1881-1891.

81. Sen, R., Zhao, B., Perea, D., Itkis, M. E., Hu, H., Love, J., Bekyarova, E., Haddon, R. C., '*Preparation of Single-Walled Carbon Nanotube Reinforced Polystyrene and Polyurethane Nanofibers and Membranes by Electrospinning'*, Nano Lett., 2004, 4, 3, 459-464.

82. Ma, M., Hill, R. M., Lowery, J. L., Fridrikh, S. V., Rutledge, G. C., '*Electrospun Poly(Styrene-block-dimethylsiloxane) Block Copolymer Fibers Exhibiting Superhydrophobicity*', Langmuir, 2005, 21, 5549-5554.

83. Aussawasathien, D., Dong, J. H., Dai, L., '*Electrospun polymer nanofiber sensors*', Synthetic Metals, 2005, 154, 37-40.

84. Stoiljkovic, A., Ishaque, M., Justus, U., Hamel, L., Klimov, E., Heckmann, W., Eckhardt, B., Wendorff, J. H., Greiner, A., '*Preparation of water-stable submicron fibers from aqueous latex dispersion of water-insoluble polymers by electrospinning*', Polymer, 2007, 48, 3974-3981.

85. Allı, A., Hazer, B., Menceloğlu, Y., Süzer, Ş., '*Synthesis, characterization and surface properties of amphiphilic polystyrene-b-polypropylene glycol block copolymers*', European Poly. J., 2006, 42, 740-750.

86. Safety Data Sheet of Tetrahydrofuran LabGrade ACS, Cat. No: 107025, date of issue: 2007, MERCK.

APPENDIX A

SAMPLE CALCULATIONS

A.1 Sample Calculation for PS/BR Blends in Tables 3.2 to 3.5

Sample calculation for PS/BR blends were given in **Appendix A** in order to make the tables more understandable. In the blend preparation part of the experiments, volume percent for both polystyrene and butyl rubber were taken but in the tables, their weight percentages were given. Therefore, the first column of each table was explained in the sample calculation and the connection between the first column and other columns were explained. The sample calculation is given below.

A.1.1 WV-20/20-90/10

WV-20/20-90/10 is explained part by part. W represents weight percentages of PS and BR solutions which are shown 20/20 (PS/BR) in this example. V represents volume percentages of PS and BR solutions are shown 90/10 (PS/BR) in this example. That is, in the preparation of this blend, 20 wt% of PS solution and 20 wt% of BR solution were used. The blend contains 90 v% of 20 wt% PS solution and 10 v% of 20 wt% BR solutions.

Given:

ρ_{PS} : 1.03 g/cm^3 (g/ml)

ρ_{BR} : 0.864 g/cm^3 (g/ml)

Basis:

100 ml of PS/BR blend solution consisting of 90 ml PS and 10 ml BR solutions

Calculation:

20 wt% PS solution in THF means 20 g PS in 100 ml THF. So the total solution amount is:

$$\frac{20\,g\,PS}{1.03\,g/ml} = 19.42\,ml\,PS$$

So the total solution becomes;

100 ml THF + 19.42 ml PS = 119.42 ml (PS + THF)

If a direct proportion balance was done;

20 g PS 119.42 ml (PS + THF)

X g PS 90.00 ml (PS + THF)

X = 15.1 g PS

20 wt% BR solution in THF means 20 g PS in 100 ml THF. So the total solution amount is:

$$\frac{20\,g\,BR}{0.864\,g/ml} = 23.23\,ml\,BR$$

So the total solution becomes;

100 ml THF + 23.23 ml BR = 123.23 ml (BR + THF)

If a direct proportion balance was done;

20 g BR 123.23 ml (BR + THF)

Y g BR 90.00 ml (BR + THF)

Y = 1.6 g BR

Therefore, 100 ml of blend solution contains 15.1 g PS and 1.6 g BR.

The total polymer concentration becomes 15.1 g + 1.6 g = 16.7 g.

APPENDIX B

GPC ANALYSIS REPORT OF POLYSTYRENE

Cirrus Sample Results Report

	LS 90				
Bulk MW:	136164			**Bulk IV:**	0.8023
MW Averages					
Mp	112750	IVp	0.782543	Rgp	11.9623
Mn	66674	IVn	0.628719	Rgn	10.0226
Mw	134676	IVw	0.793994	Rgw	12.2721
Mz	224056	IVz	0.952094	Rgz	14.4595
Mz+1	319854				
Dispersity	2.0199				

Reference Point
RT (mins):
MW:
LogM:
Weighting:

LogM - v - RT fit

$$LogM = 17.13 - 2.053\ X^{1} + 0.06348\ X^{2}$$

Calculated Mark-Houwink coefficients (calculated from selected range then extrapolated for full range)

K (antilog of intercept) = 79.5885 **Alpha (slope) =** 0.5877

Use BB parameters No

Sample Information
05/10/2007 15:30:35
Run 2, Ahmet_PS,
Batch : 05_10_2007, Filename : 05_10_2007-0001.cgrm
Type : Unknown using method triple detection